2021

Dislocation Mechanics of Total Hip Arthroplasty: A Combined Experimental and Computational Analysis

Michael Scinto
University of Denver

Dislocation Mechanics of Total Hip Arthroplasty: A Combined Experimental and Computational Analysis

Abstract

While total hip arthroplasty is considered a successful procedure, dislocation remains a serious complication as recurrent dislocations may require additional surgeries. Knowledge on dislocation events as they occur in vivo are limited, therefore researchers rely on experimental and computational methods. A custom MATLAB script and an experimental procedure utilizing a six-degree of freedom actuator were developed to further understand how various surgical considerations affect dislocation mechanics in total hip arthroplasty. Computationally, it was determined that impingement free range of motion is limited during internal rotation in flexion and during external rotation in extension. Experimentally, our results suggest that the posterior approach provides more stability to anterior dislocations as the soft tissue structures became taut sooner in the rotation. Additionally, we found that dual mobility total hip arthroplasty provided a greater resistive torque during an impingement event than conventional total hip arthroplasty.

Document Type

Thesis

Degree Name

M.S.

Department

Mechanical Engineering

First Advisor

Chadd W. Clary

Second Advisor

Paul Rullkoetter

Third Advisor

Davor Balzar

Keywords

Biomechanics

Subject Categories

Biomechanics and Biotransport | Biomedical Engineering and Bioengineering

Dislocation Mechanics of Total Hip Arthroplasty: A Combined Experimental and Computational Analysis

_____

A Thesis

Presented to

the Faculty of the Daniel Felix Ritchie School of Engineering and Computer Science

University of Denver

_____

In Partial Fulfillment

of the Requirements for the Degree

Master of Science

_____

by

Michael Scinto

June 2021

Advisor: Chadd W. Clary, PhD

Author: Michael Scinto
Title: Dislocation Mechanics of Total Hip Arthroplasty: A Combined Experimental and Computational Analysis
Advisor: Chadd W. Clary, PhD
Degree Date: June 2021

ABSTRACT

While total hip arthroplasty is considered a successful procedure, dislocation remains a serious complication as recurrent dislocations may require additional surgeries. Knowledge on dislocation events as they occur *in vivo* are limited, therefore researchers rely on experimental and computational methods. A custom MATLAB script and an experimental procedure utilizing a six-degree of freedom actuator were developed to further understand how various surgical considerations affect dislocation mechanics in total hip arthroplasty. Computationally, it was determined that impingement free range of motion is limited during internal rotation in flexion and during external rotation in extension. Experimentally, our results suggest that the posterior approach provides more stability to anterior dislocations as the soft tissue structures became taut sooner in the rotation. Additionally, we found that dual mobility total hip arthroplasty provided a greater resistive torque during an impingement event than conventional total hip arthroplasty.

ACKNOWLEDGEMENTS

I would first like to thank my advisor Dr. Chadd Clary for his mentorship and support through both my graduate and undergraduate years at the University of Denver. Additionally, I would like to thank my other committee members, Dr. Paul Rullkoetter and Dr. Davor Balzar.

I would also like to thank all of the professors and graduate students that make up the Center for Orthopaedic Biomechanics at the University of Denver. Specifically, I would like to thank Brittany Marshall for her assistance with the experimental testing and data processing, as well as Dr. Casey Myers for his assistance with the impingement free range of motion code as well as his continued guidance.

Finally, I would like to thank Ryan Keefer and the rest of the hip team at Depuy Synthes for sponsoring this work and providing the specimens and implants.

TABLE OF CONTENTS

LIST OF FIGURES

LIST OF TABLES

CHAPTER 1: Introduction

1.1 Introduction to Total Hip Arthroplasty

Total hip arthroplasty (THA) is a successful procedure in reducing pain, joint deformity, and loss of function in patients with osteoarthritis (Dowsey et al., 2016). While THA is a successful procedure, dislocation remains a complication with dislocation rates ranging from 0.12% to 16.13% (Kunutsor et al., 2019). During THA, there are many surgical considerations including approach, capsular repair, and implant selection; however, it is not clear how each of these factors affect resistance to dislocation. As the number of THA's is expected to grow from 498,000 in 2020 to 1,429,000 in 2040 (Singh et al., 2019), it is important to decrease the number of dislocations as recurrent dislocations can lead to additional surgeries (Bourne and Mehin, 2004).

Dislocation rates as a result of surgical approach are still not clear, as some studies have shown that the direct anterior approach reduces dislocation rates compared to the posterior approach (Higgins et al., 2015; Miller et al., 2018) while others have shown non-significant differences (Malek et al., 2016; Maratt et al., 2016; Tay et al., 2019). Similarly, as some surgeons perform a complete excision of the hip capsule while others perform capsular repair following THA (Swanson et al., 2019), the benefit of capsular repair is still debated. In addition to surgical approach and capsular repair

technique, dual mobility implants are gaining popularity, so it is not fully understood how all surgical considerations interact in their effects on dislocation resistance.

The goal of this thesis was to use computational and experimental methods to analyze how approach, capsular repair, and implant selection affect dislocations in total hip arthroplasty. By performing one direct anterior and posterior approach THA on contralateral hips, a repeated measures study was performed to simultaneously compare approach and effects of capsular repair. Additionally, mechanics of conventional and dual mobility total hip arthroplasty were compared as modular dual mobility allowed for implants to be swapped.

1.2 Thesis Objectives

The objectives of this this thesis were to:

1. Determine the impingement free range of motion of native hips and hips implanted with dual mobility total hip arthroplasty during internal and external rotation through flexion
2. Compare how surgical approach affects passive tissue range of motion during internal and external rotation through flexion, and compare the passive tissue constraints to the impingement free range of motion
3. Determine the relative torque contribution of capsular repair following total hip arthroplasty during internal and external rotation through flexion
4. Compare how surgical approach and capsular repair effect soft tissue stiffness and range of motion during movements likely to cause dislocations

5. Compare how dual mobility and conventional implants affect type of impingement, impingement angle, resistive torque, and resistive energy during movements likely to cause dislocations

1.3 Thesis Overview

This thesis is designed to provide both a review of previous research as well as original research related to factors which affect dislocation resistance in total hip arthroplasty. Chapter 2 provides a review of literature to give the reader insight into the methodology and research questions that have been previously investigated. Chapter 3 provides a detailed report on an original study performed at the University of Denver to analyze impingement and soft tissue mechanics of native and implanted hips during through flexion. Chapter 4 provides a detailed report on an original study performed at the University of Denver on total hip arthroplasty mechanics during movements likely to cause anterior and posterior dislocations. Chapter 5 provides concluding remarks regarding the main findings from these studies and future work.

CHAPTER 2: Literature Review

2.1 Total Hip Arthroplasty Overview

Total hip arthroplasty (THA) is a commonly performed procedure in the United States with annual counts predicted to increase from 498,000 in 2020 to 1,429,000 in 2040. (Singh et al., 2019). THA is a common treatment for patients with osteoarthritis which reduces pain, joint deformity, and loss of function (Dowsey et al., 2016). The procedure involves resecting the head/proximal neck of the femur and acetabular cartilage/subchondral bone and replacing them with a small diameter head/femoral stem and acetabular component (Siopack and Jergesen, 1995).

While THA is considered a successful procedure, dislocation as a result of impingement and levering out (Fig. 2.1) is a common reason for clinical failures (Brown et al., 2014). For primary THA, dislocation rates have been reported from 0.12% to 16.13% (Kunutsor et al., 2019). Recurrent dislocations are troublesome as they require modular components to be exchanged (i.e., change of offset, head size, etc.) or a revision surgery (Bourne and Mehin, 2004). As it remains unclear which factors affect dislocation resistance, total hip arthroplasty remains a topic of interest in biomechanical research.

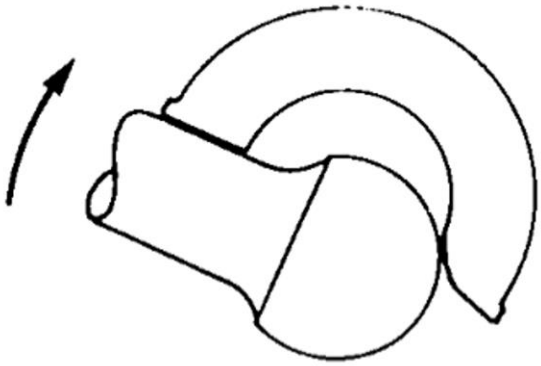

Figure 2.1: Conceptual Schematic of Impingement and Dislocation (Amstutz et al., 1975)

2.2 Dual Mobility Total Hip Arthroplasty

Dual mobility total hip arthroplasty (DM-THA) was first introduced in 1974 and was developed by Professor Gilles Bousquet and engineer André Rambert (de Martino et al., 2014). The dual mobility implant is constructed of a large-inside-diameter acetabular shell and a bipolar femoral component (Guyen et al., 2009). This design allows for two articulations: a small articulation between the femoral head/polyethylene liner and a large articulation between the polyethylene liner/acetabular shell (Blakeney et al., 2019).

Among dual mobility implants, there are two designs used for acetabular articulation and fixation. Original dual mobility technology uses a monoblock acetabular component (Fig. 2.2a) while the recently developed modified dual mobility uses an outer shell and modular liner (Fig. 2.2b) (Matsen Ko et al., 2016). One benefit of the modified dual mobility is that it allows for screw fixation, which is not available with a monoblock component (Sutter et al., 2017). Additionally, modular cup systems allow for conversion between conventional and dual mobility liners during a revision surgery.

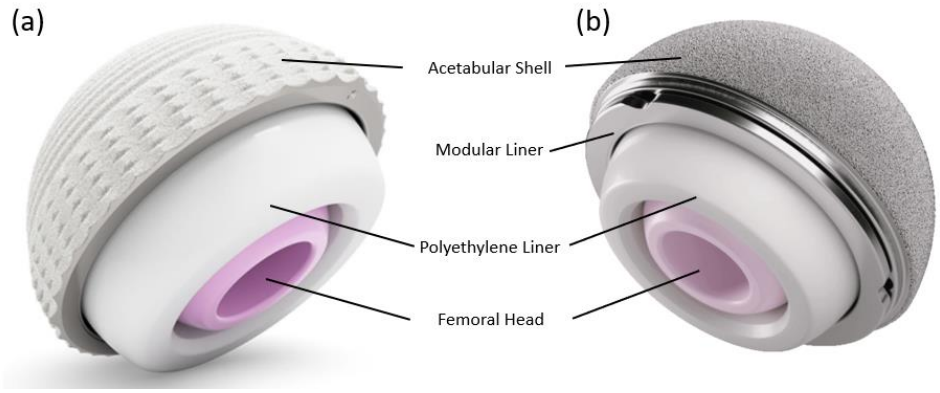

Figure 2.2. (a) Monoblock Dual Mobility (b) Modular Dual Mobility (www.jnjmedicaldevices.com)

There are many reported biomechanical advantages of DM-THA compared to conventional total hip arthroplasty (c-THA). Theoretically, the first articulation acts like a typical "hard-on-soft" bearing until the neck contacts the polyethylene, which engages the second articulation and subsequently increases the impingement free range of motion (ROM) (de Martino et al., 2014). This was proven experimentally, as dual mobility implants had larger arcs of motion in all three planes when testing femoral heads of the same size (Guyen et al., 2007). The articulating polyethylene liner also acts as a large femoral head, which increases the lateral translation necessary to dislocate (i.e., jump distance) (Sariali et al., 2009).

While there are many reported benefits to DM-THA, the complex design leads to concerns that are not applicable to c-THA. One complication of DM-THA is intra-prosthetic dislocation (IPD) which occurs when the femoral head dislocates from the polyethylene liner (Philippot et al., 2013). Philippot et al. found that IPD is due to one of the following: wear on the rim of the polyethylene liner, blockage of the polyethylene liner, or cup loosening. Due to the additional articulating surface and a thinner liner, accelerated wear is also a concern (de Martino et al., 2014). A retrieval study of 40 DM-

THA liners showed similar wear to c-THA liners, however, the rim of polyethylene liner had visible wear in 40% of the retrieved implants (Adam et al., 2014).

2.3 Surgical Approach

While there are a variety of surgical approaches to access the hip joint during THA, the posterior approach (PA) was the most common as of 2010 (Waddell et al., 2010). PA utilizes a gluteus maximum split and an incision through the posterior hip capsule and external rotators to access the hip (Fig. 2.3a) (Masonis and Bourne, 2002). The noted benefits of this approach are reduced surgery time and conservation of the gluteus medius and minimus. Additionally, it is unlikely to result in postoperative limp or abductor dysfunction.

More recently, there has been interest in the direct anterior approach (DAA) for the perceived benefits of decreased pain, faster recovery, and improved hip stability (Higgins et al., 2015). DAA requires an incision through the tensor fascia lata and anterior capsule which spares the posterior capsule and rotators (Fig. 2.3b) (Matta and Ferguson, 2005). The procedure is performed in the supine position and is generally accompanied by the use of a Judet, PROfx, or HANA table (Siguier et al., 2004; Yerasimides and Matta, 2005).

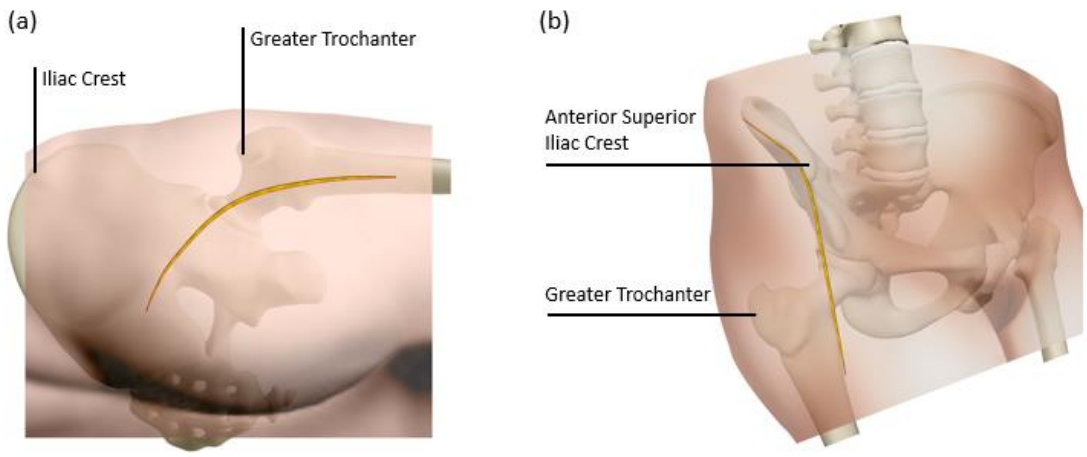

Figure 2.3: (a) Posterior Approach Incision (b) Direct Anterior Approach Incision (www.orthobullets.com)

When comparing dislocation rates between the two approaches, one approach does not clearly outperform the other. Reported dislocation rates in retrospective analyses ranged from 0.4-0.8% for DAA and 0.5-0.9% for PA (Malek et al., 2016; Maratt et al., 2016; Tay et al., 2019). While none of these studies showed statistical significance for dislocation rates, various meta-analysis have noted significant differences in favor of the anterior approach (Higgins et al., 2015; Miller et al., 2018). However, one drawback to DAA is the steep learning-curve which can range from 50-300 initial cases (Brun et al., 2018; Steiger et al., 2015).

2.4 Capsular Repair

Following total hip arthroplasty, surgeons have the choice whether or not to repair the hip capsule and other soft tissue structures. Due to surgeon preference and constant developments, there are a variety of techniques utilized during capsular repair. For a posterior capsular repair following THA, Sioen et al. (2002) noted two various methods: a soft tissue repair and a transosseous repair. The soft tissue repair involved suturing the piriformis tendon to the gluteus medius and suturing the quadratus femoris to its base,

while the transosseous repair involved suturing the posterior capsule to drill holes in the greater trochanter. It was noted that the transosseous repair closed the posterior structures "almost anatomically". Recently, a novel "noose-like" repair of the posterior capsule has shown promising results which involves tightening the repaired capsule around the prosthetic femoral neck (Swanson et al., 2019). While there is a lack of literature related to anterior capsular repair techniques, one method involved suturing the anterior capsular together and then to either the capsular cuff or osseous femur (Arac et al., 2006)

Clinically, capsular repair has shown favorable results for both the posterior and direct anterior approaches. Retrospective and meta-analyses have shown that dislocation rates following posterior approach THA ranged from 0.5-2.0% with repair and 4.0-4.8% without repair (Kwon et al., 2006; Masonis and Bourne, 2002; White et al., 2001). Only one study was found that reported dislocation rates following an anterior capsular repair; however, 0 of the 32 hips dislocated within their one-year follow up (Arac et al., 2006) Capsular repair has also been shown to be effective in revision THA as dislocation rates of 3.0% and 21.4% were reported for repaired and unrepaired capsules, respectively (Jurkutat et al., 2018).

It has been shown experimentally that more rotation is required to dislocate a hip with a repaired capsule than an unrepaired capsule which is likely the key factor in reducing dislocation rates. In a cadaveric study, it was shown that the transosseous repair provided significantly more rotation to dislocation when compared to a soft tissue repair or no repair (Sioen et al., 2002). Similarly, it was found that the novel "noose-like" technique provided significantly more rotation to dislocation when compared to a classic repair or no repair (Swanson et al., 2019). In both cases, the soft tissue and classic repair

provided more rotation to dislocation than no repair, however, the differences were not statistically significant. As the majority of capsular repair research focuses on posterior repairs, the increasing interest in the direct anterior approach suggest that research on anterior repairs would provide clinical benefit.

2.5 Overview of Dislocation Following Total Hip Arthroplasty

While studies have noted spontaneous dislocation of the prosthetic hip, dislocations are most frequently caused by an impingement event which levers the femoral head out of the acetabular socket (Bartz et al., 2000). Impingement can occur between either the femoral stem/acetabulum liner, femur/pelvis, femoral stem/pelvis, or between the femur/acetabular liner (Palit et al., 2020). During an impingement event, there is a large buildup of stress at the impingement site as well as on the egress side (Fig. 2.4) (Brown et al., 2014). As the stem continues to rotate about the impingement fulcrum, the egress site provides a resisting moment created by compressive and frictional stresses which resists the head levering out (Scifert et al., 2001). Dislocation occurs when the egress side fails to resist egress of the femoral head (Dorr, 2014).

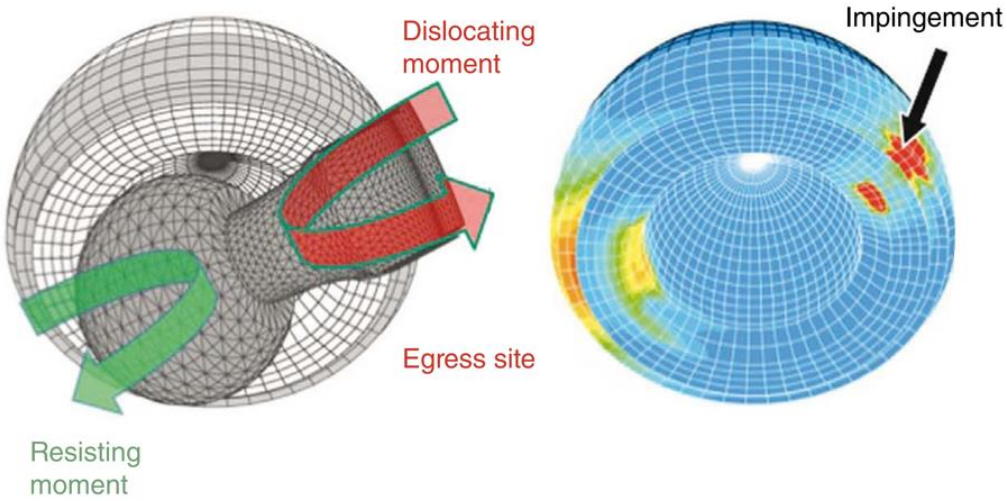

Figure 2.4. Finite Element Schematic of Impingement and Dislocation (Dorr 2014)

Hip dislocations are classified by the direction in which the femoral head egresses, either anterior or posterior. Anterior dislocations can result from combined extension, abduction, and external rotation while posterior dislocations can result from combined flexion, adduction, and internal rotation (Dawson-Amoah et al., 2018).

To analyze which movements result in anterior and posterior dislocations, researchers have utilized computational studies as well as anecdotes from patients who have suffered dislocations. Using experimental kinematic data as the input, a finite element analysis discovered that rolling over while lying down and pivoting were likely to result in anterior dislocations, while sit-to-stand maneuvers and tying shoes while seated were likely to result posterior dislocations (Nadzadi et al., 2003). Anecdotes from 1202 patients who suffered dislocations following THA showed similar results to the computational study. A majority of the anterior dislocations occurred in bed or while pivoting, whereas the majority of posterior dislocations occurred while sitting and performing activities of daily living (ADLs) such as gardening and household chores (Pedersen et al., 2005).

2.6 Previous Research Surrounding Impingement Free ROM

To study the impingement free ROM of hips implanted with THA, researchers utilize computational and experimental methods. Early computational models would rotate the femoral stem about a desired axis until a collision with the liner was detected (D'lima et al., 2000), whereas later models began including bony geometries in the collision algorithm (Kessler et al., 2008). Methodology for the experimental studies varies greatly, as methods to rotate the hip have included manual rotation (Fig. 2.5a), the use of cables to simulate muscles (Fig. 2.5b), and 6 degree-of-freedom robots (Fig. 2.5c).

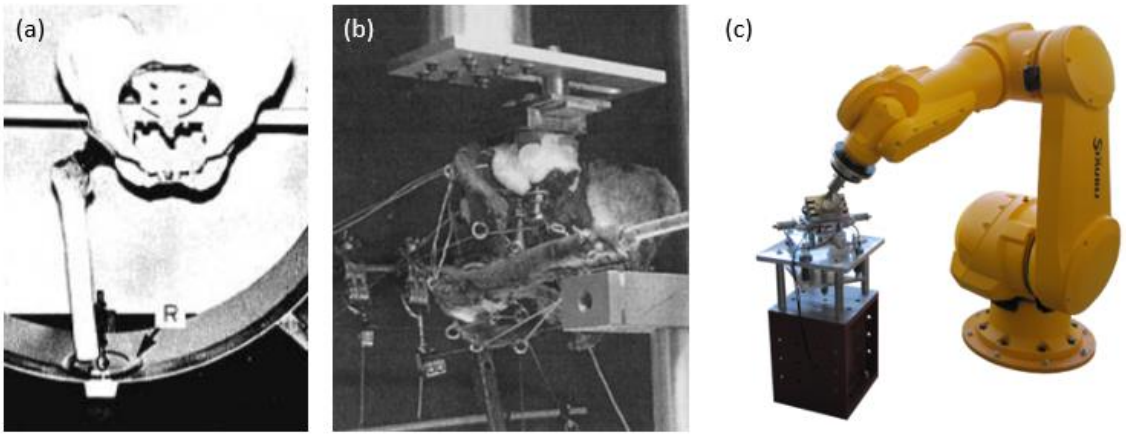

Figure 2.5: (a) Manual Femoral Rotation (Amsturtz et al., 1975) (b) Femoral Rotation via. Cables (Scifert et al., 2001) (c) Robotic Femoral Rotation (Hermann et al., 2015)

As the Lewinnek safe zone of 15 ± 10° of anteversion and 40 ± 10° of inclination is commonly targeted for acetabular cup placement (Fig. 2.6) (Lewinnek et al., 1978), computational models have been used to analyze how alternate component positioning affects impingement free ROM. When only looking at component impingement (i.e., no bony geometries), it was found that acetabular inclination angles less than 45 degrees decreased flexion and abduction while angles greater than 45 degrees decrease adduction and axial rotation (D'lima et al., 2000). Additionally, increasing the anteversion of the acetabular component provided a greater impingement free ROM in flexion (Scifert et al., 2001). A common finding among all studies was that increasing head size increased impingement free ROM (D'lima et al., 2000; Kessler et al., 2008; Scifert et al., 2001).

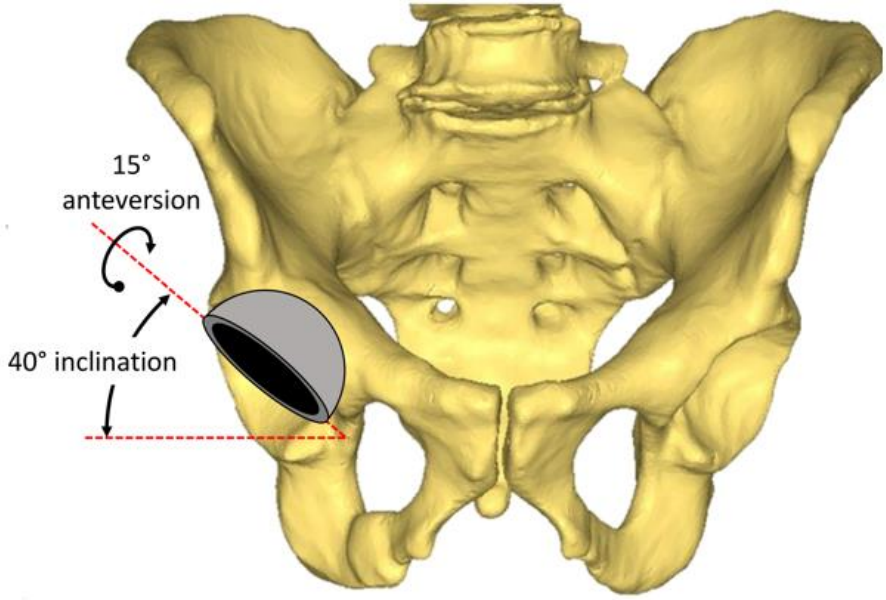

Figure 2.6: Schematic of Acetabular Cup Positioning in the Lewinnek Safe Zone

Limitations of the early models became evident as experimental and computational methods improved. When bony geometries were incorporated into the models, it was found that bony impingement decreased ROM in 44% of motions tested (Kessler et al., 2008). Furthermore, studies begun combining virtual simulations with experimental studies using the same specimens (i.e., a matched pair) (Incavo et al., 2011). This was done because impingement driven by implant, bone, and soft tissue become less important if they occur at rotations that the patient cannot reasonably achieve. Utilizing this methodology, the soft tissue structures in native hips such as muscles, capsule, labrum, and ligaments were shown to restrict ROM even further than bony impingement alone (Han et al., 2020).

2.7 Previous Research Surrounding Dislocation Resistive Torques

To understand how soft tissue structures and implants affect torque responses, researchers have utilized finite element models and experimental studies. In general, the

finite element models are calibrated by running a few experimental simulations and tuning the model to analyze implant and soft tissue effects (Kluess et al., 2007; Scifert et al., 2001). Experimentally, one methodology involves applying a consistent torque and measuring ROM (Lgoishetty et al., 2019; van Arkel et al., 2018) while the other methodology involves applying a rotation and measuring torque (Mihalko and Whiteside, 2004; Sioen et al., 2002; Swanson et al., 2019).

With the finite element models, it was found that an increase in the liner lip chamfer angle and cup center offset increased the resistive moment, while an increase in lip breadth decreased the resistive moment (Fig. 2.7) (Scifert et al., 2001). Additionally, increasing the head size was found to have two benefits: increased resistive moment and decreased contact stress (Kluess et al., 2007). When the hip capsule was incorporated into the models, it was found that capsule compromise was the dominant factor in hip instability (Elkins et al., 2011). Furthermore, thigh-thigh contact was found to have an effect on dislocations in patients with higher BMIs, when muscle, adipose tissue, and skin were included in the model (Elkins et al., 2013).

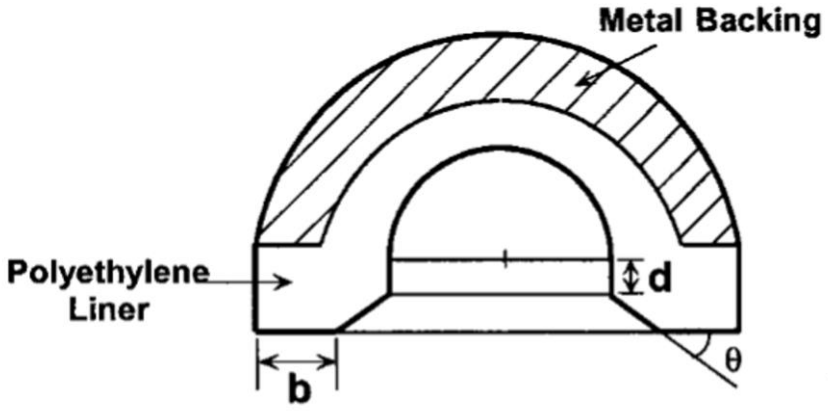

Figure 2.7: Schematic of Acetabular Liner Design Variables. θ: Chamfer Angle, b = Lip Breadth, d = Cup Center Inset (Scifert et al., 2001)

When observing the effect of capsular repair during THA, experimental studies showed that a transosseous repair provided significantly more torque at the time of dislocation than either a soft tissue repair or no repair at all (Mihalko and Whiteside, 2004; Sioen et al., 2002). A later study found that their novel "noose-like" technique (described previously) provided significantly more torque than the transosseous repair (Swanson et al., 2019). When comparing the effects of surgical approach, it was found that the PA had decreased ROM in extended positions while the DAA had decreased ROM in flexed positions (Lgoishetty et al., 2019).

While the study's reviewed here provide insight into mechanics of resistive torques following THA, some of the mechanics are still not fully understood. For example, one study has shown that increasing femoral head size increases resistive torque (Kluess et al., 2007), while other studies have shown DM-THA reduces resistive torque (Klemt et al., 2020; Terrier et al., 2017). As DM-THA has a larger effective head than the c-THA heads tested, it would have been expected that resistive torque would increase for DM-THA. Additionally, there is a general lack of research on benefits of anterior capsular repair. Therefore, there would be clinical benefit in testing how surgical approach, capsular repair, and implant affect resistance to movements likely to cause both anterior and posterior dislocations.

CHAPTER 3: Impingement and Soft Tissue Mechanics of Native and Implanted Hips Through Flexion

3.1 Introduction

Impingement can lead to major concerns in both native hips and hips implanted with total hip arthroplasty (THA). In native hips, femoroacetabular impingement (FAI) has been found to be a precursor to osteoarthritis (Leunig and Ganz, 2014). In implanted hips, impingement can cause dislocation as it levers the femoral head out of the acetabular socket (Scifert et al., 1999). Knowledge of these impingement events as they occur *in vivo* are limited, therefore researchers rely on computational simulations (D'lima et al., 2000; Kessler et al., 2008) and cadaveric studies (Bartz et al., 2000; Burroughs et al., 2005).

FAI in native hips can be defined as either cam impingement, pincer impingement, or both (Pfirrmann et al., 2006). Cam FAI is a result of a non-spherical femoral head and reduced depth of the femoral waist while pincer FAI is a result of acetabular over-coverage. In both cases, the impingement free range of motion (ROM) is less than that of healthy hips.

Impingement in implanted hips is multifactorial as it depends on the patient's anatomy as well as surgical considerations. The Lewinnek safe zone is commonly targeted for acetabular component placement to prevent dislocations (Lewinnek et al.,

1978), however, this safe zone is highly debated (Esposito et al., 2015). More recently, dual mobility total hip arthroplasty (DM-THA) has been introduced as an attempt to decrease dislocation frequency. It has been shown experimentally that dual mobility implants have larger arcs of motion in all three planes when testing femoral heads of the same size (Guyen et al., 2007).

While there are a variety of surgical approaches to access the hip during THA, multiple studies have focused on comparing stability between the direct anterior approach (DAA) and posterior approach (PA) (Maldonado et al., 2019; Malek et al., 2016; Maratt et al., 2016). As of 2010, PA was the most common (Waddell et al., 2010) and its associated benefits include reduced surgery time and conservation of the gluteus medius and minimus (Masonis and Bourne, 2002). However, DAA has recently gained popularity for the perceived benefits of decreased pain, faster recovery, and improved hip stability (Higgins et al., 2015). Retrospective analyses have shown that dislocation rates remain similar between the two approaches, ranging from 0.4-0.8% for DAA and 0.5-0.9% for PA (Malek et al., 2016; Maratt et al., 2016; Tay et al., 2019).

During THA, some surgeons perform a complete excision of the capsule while others perform capsular repair (Swanson et al., 2019), therefore it is important to understand the effects each have on stability of the prosthetic hip. Retrospective and meta-analyses have shown that dislocation rates following a posterior approach total hip arthroplasty range from 0.5-2.0% with repair and 4.0-4.8% without repair (Kwon et al., 2006; Masonis and Bourne, 2002; White et al., 2001). While clinical studies generally focus on effects of posterior capsular repair, one study performed 32 hip replacements

with an anterior capsular repair and had 0 dislocations within their one-year follow up visit (Arac et al., 2006).

The first goal of this study was to use a computational simulation to analyze types of impingement and the impingement ROM in native and DM-THA hips. The second goal was to experimentally determine the range of motion constraints following anterior and posterior capsule repairs. The final goal was to experimentally determine the relative torque contribution the sutures provide during various rotations.

3.2 Methods

Specimen Preparation:

Five fresh-frozen pelvis-to-toe cadaveric specimen (10 hips) underwent bi-lateral DM-THA with capsular repair performed by ten different practicing orthopaedic surgeons. Surgery on the first side was performed using the PA while the contralateral side was performed using DAA. The pelvises were implanted with PINNACLE® DM-THA while the femurs were implanted with CORAIL® or SUMMIT® stems (Depuy-Synthes, Warsaw, IN). Specimen information including component types and positioning are reported in Table 3.1. All specimens underwent pre- and post-operative CT scans to measure the native anatomy and bone-implant relative alignment. 3D models of the native femur/pelvis, implanted femur/pelvis, femoral stem, and acetabular shell were created for each hip using ScanIP (Synopsys, Mountain View, CA).

Table 3.1: Specimen Information

	Anterior Approach n=5	**Posterior Approach n=5**
Femoral Component	Corail n=2 Summit n=3	Corail n=5
Acetabular Component	Pinnacle n=5	Pinnacle n=5
Acetabular Inclination	44.0 ± 6.1°	46.8 ± 3.1°
Acetabular Anteversion	25.4 ± 3.1°	28.6 ± 7.0°
Femoral Anteversion	17.6 ± 13.4°	25.6 ± 9.9°

Pelvic and femoral coordinate systems were created from the native pelvic and femoral 3D models, respectively (Fig. 3.1). The pelvic coordinate system was defined by the anterior pelvic plane (APP) constructed with both anterior superior iliac spines (ASIS) and the pelvic tubercle midpoint (PTM). The left and right ASIS landmarks were used to align the APP in the coronal plane. The femoral coordinate system was defined by the mechanical axis constructed with the femoral epicondyle midpoint (FEM) and the center of the femoral head. The posterior aspects of the femoral condyles were used to align the femoral mechanical axis in the transverse plane. These coordinate systems were defined in prior studies (Tannast et al., 2007). The center of curvature of both the acetabulum and femoral head were used to define the origin of each coordinate system. The 3D models of the implanted femur, pelvis, and respective implants were aligned to the native bones, with CAD implant models aligned to the scanned implants.

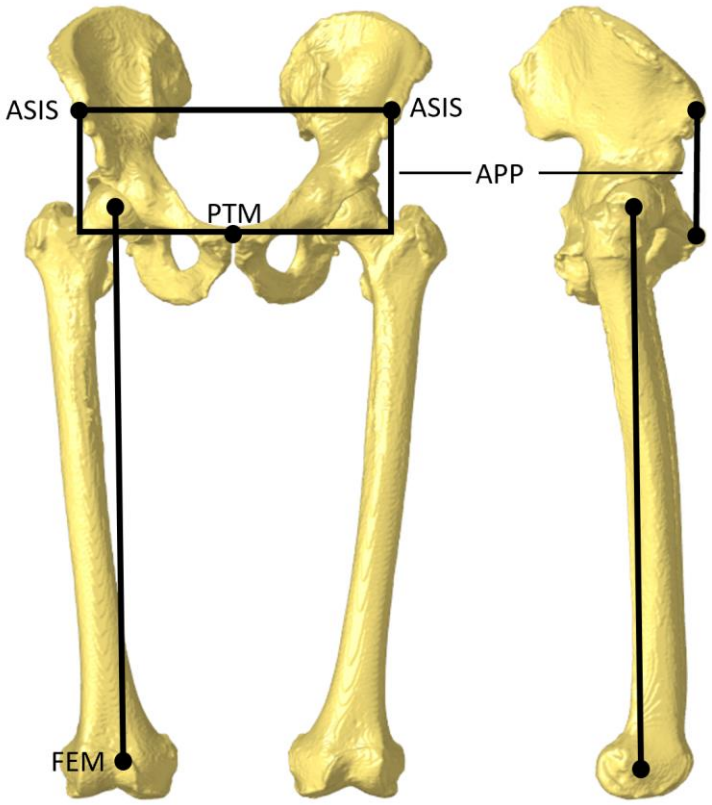

Figure 3.1: Pelvic and Femoral Coordinate Systems

Impingement Free ROM:

To determine impingement free ROM, collisions were detected with the MATLAB function 'fastmesh2mesh' (Seers, 2021) which was developed based on the 'ray triangle intersection' algorithm (Möller and Trumbore, 1997). The hip was rotated about the superior-inferior axis (i.e., internal/external rotation) at 1 degree increments while the simulation checked for impingement. This process was repeated at flexion angles from 30° of hyperextension to 120° of flexion, at 10° increments. In the native hip, collisions were detected between the femoral neck and acetabular rim (i.e., FAI, Fig. 3.2a). In the implanted hip, collisions were detected between the femoral stem and acetabular liner (i.e., component-component, Fig. 3.2b), femoral stem and osseous

acetabulum (i.e., component-bone, Fig. 3.2c) and between the remaining femur and pelvis (i.e., bone-bone, Fig. 3.2d). The segmented pelvis and femur were meshed with approximate 2 mm triangular-elements while the implants were meshed with approximate 1 mm triangular-elements.

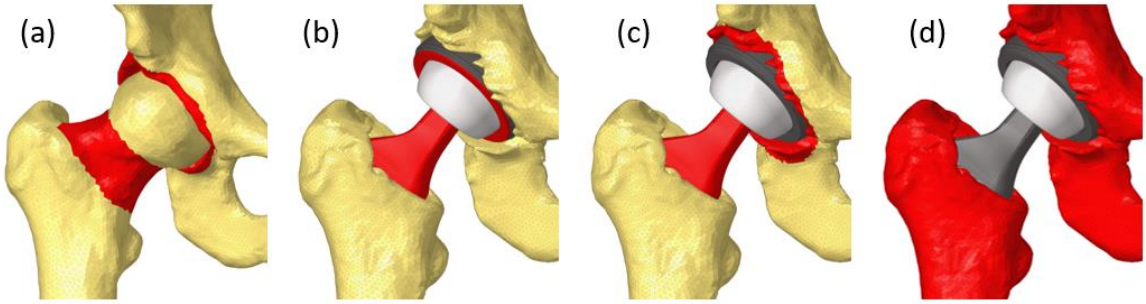

Figure 3.2: (a) FAI (b) Component-Component Impingement (c) Component-Bone Impingement (d) Bone-Bone Impingement

Experimental Laxity Testing:

An AMTI VIVO Six Degree of Freedom (DOF) Joint Simulator (AMTI, Watertown, MA) (Fig. 3.3) was used to apply forces and torques to the hip while measuring translations and rotations. The pelvis was mounted to a specimen specific 3D printed fixture while the femur was mounted inside of a cylindrical fixture with set screws and bone cement. This aligned the pelvis and femur to the previously defined coordinate systems and ensured the hip center of rotation was coincident with the rotational degrees of freedom of the actuator. An auxiliary motion capture system (Optotrak Certus™, NDI, Ontario, Canada) was used to track rigid arrays of infrared emitting diodes (IRED) on the pelvis and femur. The use of the optical tracking system was used to calculate errors in fixturing.

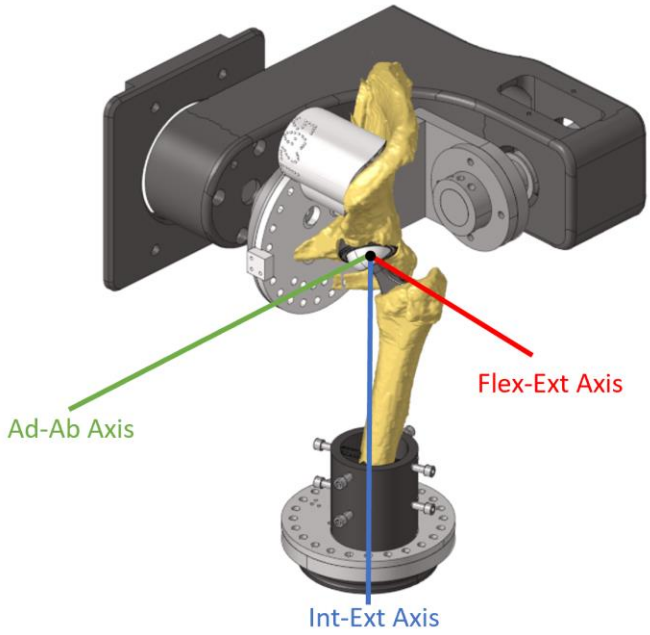

Figure 3.3: Hip Mounted in the AMTI VIVO 6 DOF Actuator with Labeled Rotational Axes

Internal and external rotation laxity assessments were performed at 4 flexion angles (0°, 30°, 60°, 90°) under two conditions: sutures intact and removed, to calculate the relative contribution of the capsular repair. A 50 N compressive load and 10 N medial load were applied to the hip via the femur keep the implants in contact while the anterior-posterior load was set to 0 N. The flexion-extension and adduction-abduction axes were set to 0 Nm of torque-control and the internal-external axis was loaded with a trapezoidal wave with a peak of 5 Nm. This value has been previously used to describe a taut hip capsule (van Arkel et al., 2015).

When the laxity trials were complete, the hips were skeletonized and 4 fiducial markers with 3 mm hemispherical indents were screwed into pelvis and femur, respectively. The fiducial markers were digitized using the motion capture system to measure the relative alignment between the fiducial markers and the IRED arrays. The

femur and pelvis were then white-light scanned using a Space Spider 3D Scanner (Artec, Luxembourg City, Luxembourg).

Post Processing

The white-light scans of the skeletonized DM- and c-THA femur and pelvis were converted into 3D models and aligned to the original CT 3D models in their anatomical position. This orientation defined neutral rotation and translation and aligned the experimental and computational coordinate systems. Experimental kinematics were calculated by adding the "fixturing offset" (measured by the motion capture) to rotations measured by the VIVO while forces and torques were recorded using a load-cell mounted below the femur.

Torque-rotation curves were plotted for each trial and used to calculate the passive tissue envelope and suture contribution. Both torque and rotation were each calculated about the superior-inferior femoral axis. Not all specimens reached 5 Nm of torque before hitting mechanical limits on the simulator, therefore, 2 Nm was used as the peak torque as this value was used previously in similar studies (Mihalko and Whiteside, 2004). The angle at which the sutures intact hip reached a 2 Nm torque was defined as the end of the passive tissue envelope. At this same angle, the torque recorded during the sutures removed case was used to determine the relative suture and capsule contribution (Fig 3.4). The relative suture and capsule contribution were calculated as a percentage of the total 2 Nm of torque.

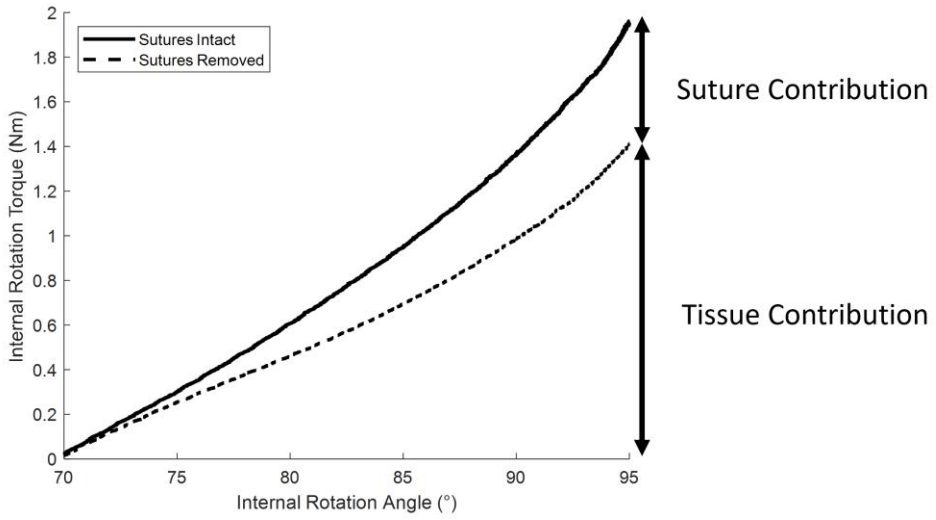

Figure 3.4: Torque-Rotation Curve Showing Relative Suture and Tissue Torque Contribution

Statistical Analysis

A 2-way repeated measures analysis of variance (ANOVA) with a Tukey's post-hoc test was used to test statistical significance for each comparison. Flexion angle and impingement condition were independent factors for the impingement free ROM analysis, while flexion angle and approach were independent factors for the passive 2 Nm envelope and suture contribution analysis. The significance level was set at $p < 0.05$.

3.3 Results

Impingement Free ROM:

Through flexion, the impingement free ROM decreased for internal rotation (Fig. 3.5a) and increased for external rotation (Fig. 3.5b). For ease of comparison, internal and external impingement angles are displayed at 0°, 30°, 60°, and 90° of flexion.

During internal rotation, the native hips had mean impingement angles of 105.7 ± 20.0°, 86.2 ± 15.3°, 46.7 ± 9.5°, and 26.5 ± 11.4° for flexion angles of 0°, 30°, 60°, and 90°, respectively. The native hips had a statistically significant smaller impingement free

ROM than each of the implanted conditions. The implanted conditions with the smallest impingement free ROM were bone-bone (135.0 ± 16.8°), component-bone (125.1 ± 20.2°), bone-bone (70.9 ± 18.5°), and bone-bone (46.7° ± 19.5) for flexion angles of 0°, 30°, 60°, and 90°, respectively. Differences between types of impingement in the implanted hip were generally not statistically significant, however, bone-bone impingement free ROM was significantly smaller than component-component at 60° of flexion.

During external rotation, the native hips had mean impingement angles of 26.6 ± 12.6°, 49.5 ± 15.8°, 82.7 ± 23.1°, and 95.8 ± 8.6° for flexion angles of 0°, 30°, 60°, and 90°, respectively. The native hips generally impinged prior to the implanted hip, but only had a significantly smaller impingement free ROM than component-component impingement at 30° of flexion. The implanted conditions with the smallest impingement free ROM were component-component (38.0 ± 21.2°), bone-bone (49.7 ± 22.7°), bone-bone (95.2 ± 16.9°), and component-bone (105.9 ± 11.9°) for flexion angles of 0°, 30°, 60°, and 90°, respectively. Bone-bone impingement free ROM was significantly smaller than component-component and component-bone at 30° flexion, and component-bone at 60° of flexion.

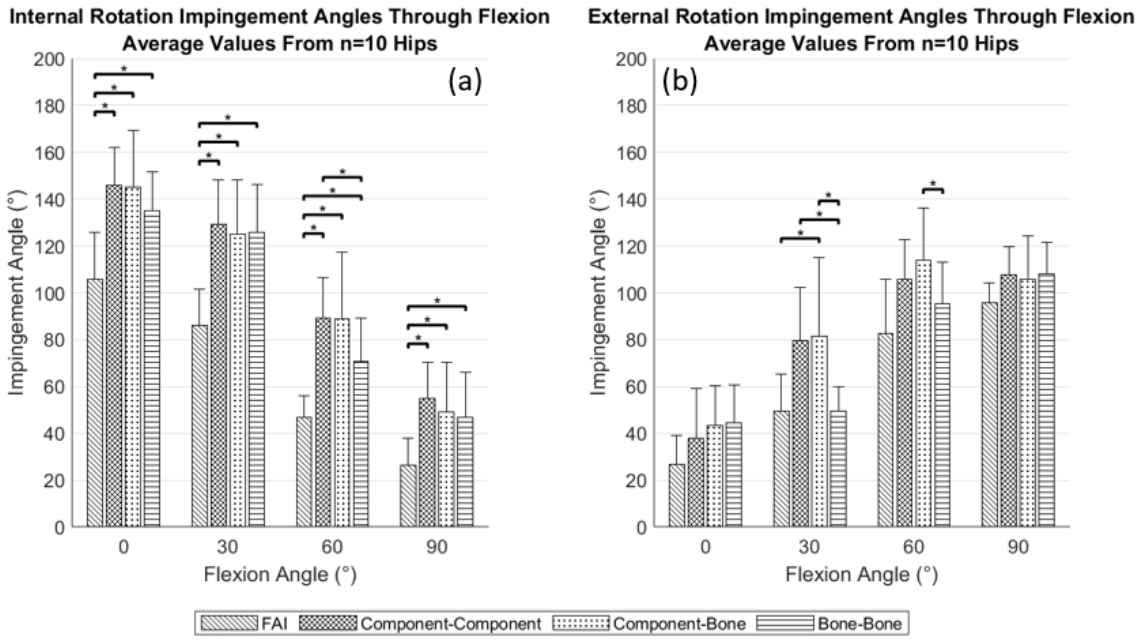

Figure 3.5: (a) Internal Rotation Impingement Angles (b) External Rotation Impingement Angles

Experimental Laxity Testing:

The sutures intact, passive tissue envelope was tightest for internal rotation in deep flexion and for external rotation in full extension (Fig. 3.6). The mean 2 Nm passive tissue envelope was within the mean computationally predicted impingement free ROM for all cases except for internal rotation at 90° of flexion for the PA specimens. Across all specimens, this was the only rotation where the 2 Nm passive tissue response ever occurred outside of the impingement free ROM.

In internal rotation, the DAA specimens reached 2 Nm at 69.6 ± 13.1°, 68.0 ± 18.0°, 51.1 ± 19.2°, and 32.0 ± 20.0°, while the PA specimens reached 2 Nm at 51.3 ± 14.3°, 61.5 ± 19.9°, 53.9 ± 18.5°, 43.9 ± 16.5° at flexion angles of 0°, 30°, 60°, and 90°, respectively. The PA specimens had a tighter passive tissue envelope at 0° and 30°, while the DAA specimens has a tighter passive tissue envelope at 60° and 90° of flexion. None

of the differences between the DAA and PA means were statistically significant for internal rotation.

In external rotation, the DAA specimens reached 2 Nm at 18.8 ± 10.8°, 20.7 ± 10.2°, 31.5 ± 7.3°, and 34.6 ± 13.1°, while the PA specimens reached 2 Nm at -8.9 ± 10.1°, 11.3 ± 13.1°, 18.6 ± 14.2°, and 22.5 ± 15.3° at flexion angles of 0°, 30°, 60°, and 90°, respectively. The PA specimens had a tighter passive tissue envelope at all flexion angles, with a statistically significant difference at 0° flexion.

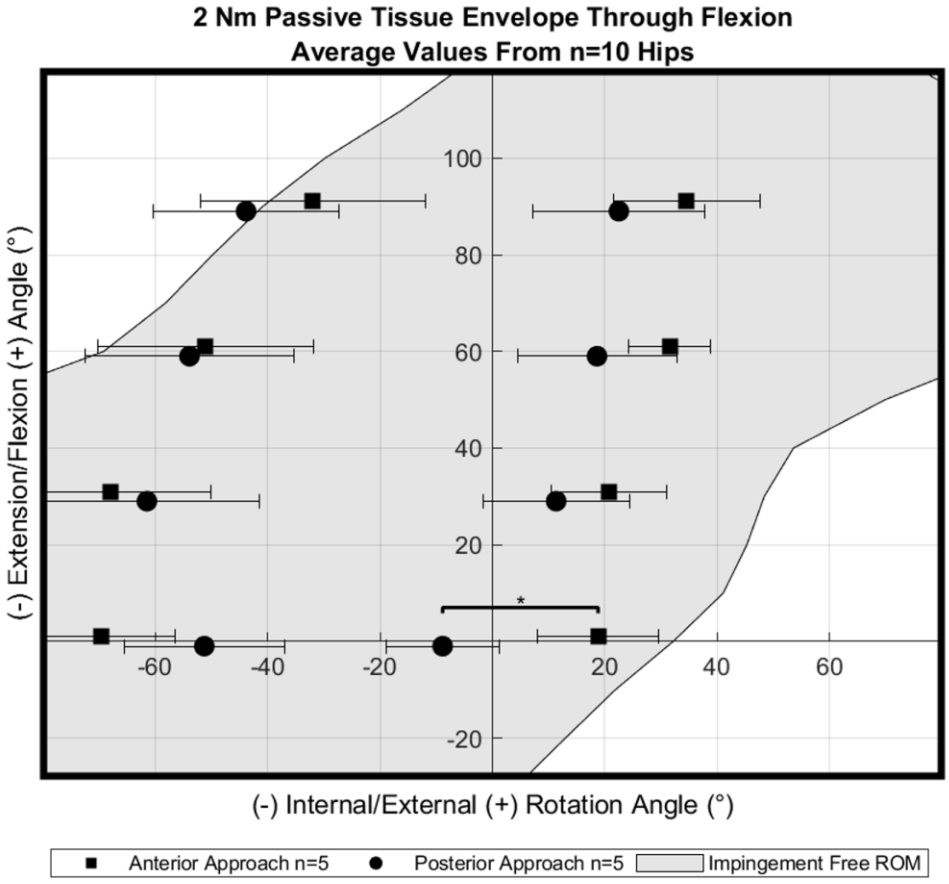

Figure 3.6: 2 Nm Passive Tissue Envelope Overlaid with Impingement Free ROM

In internal rotation, the mean suture contribution for the DAA specimens was 40.0% ± 15.8%, 42.6% ± 14.9%, 36.3% ± 21.4%, and 29.2% ± 34.7% at flexion angles of

0°, 30°, 60°, and 90°, respectively. The mean suture contribution for the PA specimens was 42.8% ± 27.5%, 61.4% ± 26.5%, 43.8% ± 27.3%, and 34.3% ± 27.3% at flexion angles of 0°, 30°, 60°, and 90°, respectively. (Fig. 3.7a). The posterior repair provided more torque than the anterior repair at all flexion angles, however, none of the differences were statistically significant.

In external rotation, the mean suture contribution for the DAA specimens was 31.9% ± 23.2%, 15.3% ± 12.5%, 30.7% ± 27.7%, and 42.6% ± 22.3% at flexion angles of 0°, 30°, 60°, and 90°, respectively. The mean suture contribution for the PA specimens was 24.0% ± 17.8%, 25.9% ± 26.0%, 21.9% ± 26.0% and 29.9% ± 14.4% at flexion angles of 0°, 30°, 60°, and 90°, respectively (Fig. 3.7b). The anterior repair sutures provided more torque than the posterior repair sutures at all flexion angles except for 30° flexion, however, none of the differences were statistically significant.

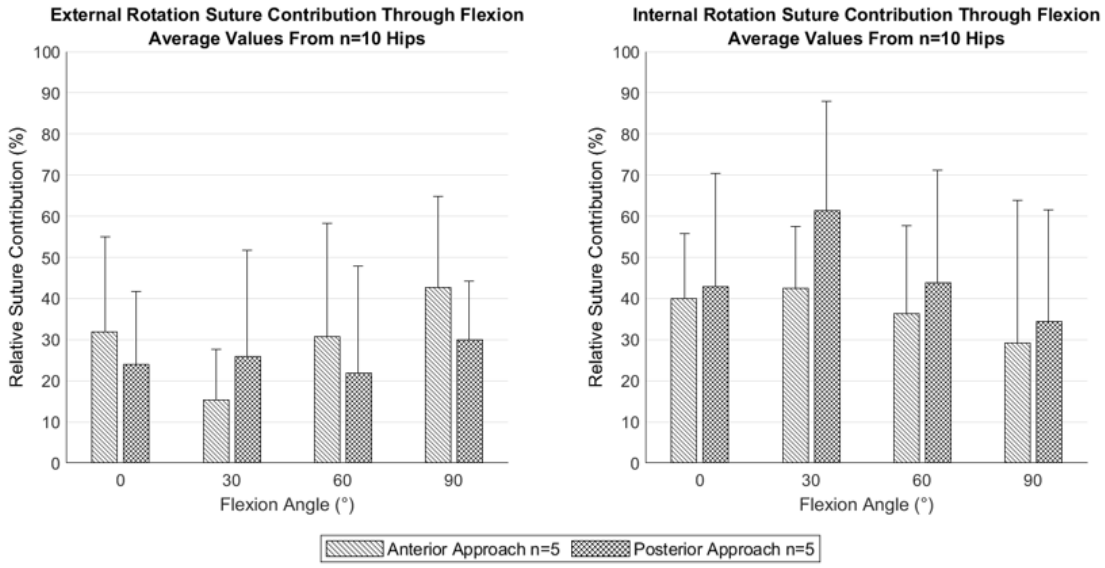

Figure 3.7: (a) Internal Rotation Suture Contribution (b) External Rotation Suture Contribution

3.4 Discussion

While computational studies provide useful information on impingement free ROM, they generally do not account for soft tissue effects. By experimentally testing the same cadaveric specimens used as 3D models in the computational analysis, we were able to analyze how passive tissues further limit range of motion.

In native hips, impingement free ROM decreased for internal rotation through flexion and increased for external rotation through flexion. This same trend was found in a previous study which utilized a CT-based, impingement free ROM analysis for native hips (Tannast et al., 2012). Furthermore, during internal rotation at 90° flexion, females have been found to a have significantly larger impingement free ROM suggesting that males are at higher risk of FAI during this movement (Nakahara et al., 2011).

The implanted hips showed the same trend as the native hips, with impingement free ROM being smallest during internal rotation at 90° flexion and external rotation at 0° flexion. In addition to pure flexion, these two movements are likely to cause impingement in implanted hips during activities of daily living (Burroughs et al., 2005). Experimental analyses have also shown that as femoral head diameter increases, so does the frequency of bone-bone impingement (Bartz et al., 2000; Burroughs et al., 2005). Bone-bone was the most common impingement type as it occurred first for 45% of the trials, compared to 32.5% and 22.5% for component-component and component-bone impingement, respectively. This supports the notion that the articulating liner in DM-THA acts as a large femoral head.

When comparing impingement in native hips to impingement in implanted hips, FAI had the smallest mean impingement free ROM for each flexion angle during both

internal and external rotation. In internal rotation, this trend was true in all cases except for one specimen which had component-bone impingement prior to FAI during internal rotation at 90° flexion. However, in external rotation there were three specimens who had implanted impingement prior to natural impingement at all four flexion angles. These three specimens had significantly greater femoral version and combined version than the other seven specimens ($p = 0.004$ and $p = .002$, respectively, 2-sample t-test). Results from other studies had similar findings as an increase in femoral version was shown to decrease impingement free ROM for external rotation at 0° flexion and increase impingement free ROM for internal rotation at 90° flexion (Burroughs et al., 2005).

When passive tissues become taut, they minimize total range of motion and may prevent the hip from reaching an impinged position. Rotations at which the predicted impingement angles were close to the passive tissue envelope (i.e., at risk of impingement) included internal rotation at 90° of flexion and external rotation at 0° of flexion. While not statistically significant, the mean values suggest that internal rotation at 90° of flexion was more likely to impinge for the PA specimens while external rotation at 0° was more likely to impinge for the DAA specimens. This supports previous findings in which PA specimens were found to have a larger range of motion in flexion while DAA were found to have a larger range of motion in extension (Lgoishetty et al., 2019).

For internal rotation at 90° of flexion, we saw a slightly greater relative suture contribution for the posterior approach which suggests that during this motion, the posterior capsule was in tension. Conversely, for external rotation at 0° of flexion, we saw a slightly greater relative suture contribution for the anterior approach which suggests that the anterior capsule was in tension. For both of these rotations at risk of

impingement, a greater range of motion was allowed when the sutures were removed which further increases risk of impingement.

While this study provides some useful insight into impingement free ROM and passive tissue responses, there were a few limitations. Along with a small sample size, all surgeries were performed by different orthopaedic surgeons using their own surgical technique and choice of implant/sizing, therefore, a large variance was seen across the specimens. An additional source of error in some specimens was due to soft tissue structures wrapping around the implants or bony landmarks in between trials, as some cases showed a greater torque without sutures than with the sutures.

The results from this study highlight a few clinically relevant findings. Knowing that internal rotation is at risk of impingement in flexion while external rotation is at risk of impingement is useful in surgical planning. Furthermore, the combined increase of acetabular and femoral version may lead to earlier impingement during external rotation. The results also show that surgical approach has effects on directional stability and that capsular repair may be beneficial in resisting excessive rotation.

CHAPTER 4: Total Hip Arthroplasty Mechanics During Movements Likely to Cause Anterior and Posterior Dislocations

4.1 Introduction

While total hip arthroplasty (THA) is considered a successful procedure, dislocation remains a common complication with dislocation rates ranging from 0.12% to 16.13% (Kunutsor et al., 2019). Dislocation as a result of impingement and levering out is a common reason for clinical failures (Brown et al., 2014). Knowledge of hip dislocations as they occur *in vivo* are limited, therefore researchers rely on computational simulations (Elkins et al., 2011; Scifert et al., 2001, 1999) and cadaveric studies (Bartz et al., 2000; Lgoishetty et al., 2019).

Hip dislocations are classified by the direction in which the femoral head egresses, either anterior or posterior. Anterior dislocations can result from combined extension, abduction, and external rotation while posterior dislocations can result from combined flexion, adduction, and internal rotation (Dawson-Amoah et al., 2018). Rolling over while lying down and pivoting while standing are likely to cause anterior dislocations, while sit-to-stand maneuvers and tying shoes while seated are likely to cause posterior dislocations (Nadzadi et al., 2003).

Prior to impingement, the soft tissues of the hip play a role in resisting movement and preventing the hip to reach vulnerable positions. Factors which may affect the torque

response of the hip include surgical approach and capsular repair. The posterior approach (PA) and direct anterior approach (DAA) are two common surgical approaches with various associated benefits; however, clinically they have shown similar dislocation rates (Malek et al., 2016; Maratt et al., 2016; Tay et al., 2019). Repair of the posterior capsule has shown a significant decrease in dislocation rates repair (Kwon et al., 2006; Masonis and Bourne, 2002; White et al., 2001), but little research has been done on the clinical benefits of capsular repair following a direct anterior approach surgery.

In addition to soft tissue, implant design plays a large role in dislocation mechanics. Currently dual mobility (DM-THA) is becoming one the of most popular designs to manage unstable THA (Guyen, 2016). One main benefit of DM-THA is additional impingement free range of motion (ROM) in comparison to conventional implants (c-THA) which has been proven *in vitro* (Guyen et al., 2007). During an impingement event, it has been shown that DM-THA decreases the resistive torque which may prevent wear, mechanical failure, or implant loosening (Klemt et al., 2020; Terrier et al., 2017). Additionally, the larger effective head of the articulating liner in DM-THA mathematically requires a greater lateral translation to dislocation (i.e., greater jump distance) (Sariali et al., 2009).

The first goal of this study was to analyze surgical technique effects, by experimentally comparing how surgical approach (i.e., DAA/PA) and technique (i.e., sutures intact/removed) effect soft tissue stiffness and passive range of motion. The second goal was to compare DM- and c-THA implant mechanics by experimentally comparing types of impingement and impingement angles, as well as resistive torque and resistive energy.

4.2 Methods

Previously Established Methodology:

Five fresh-frozen cadaveric specimens (10 hips) underwent bi-lateral DM-THA with one PA and one DAA on contralateral hips. The pelvises were implanted with PINNACLE® DM-THA while the femurs were implanted with CORAIL® or SUMMIT® stems (Depuy-Synthes, Warsaw, IN). 3D models were created using pre- and post-operative CT scans and the anatomies were aligned to an anatomical coordinate system. An AMTI VIVO Six Degree of Freedom (DOF) Joint Simulator (AMTI, Watertown, MA) (Fig. 4.1) was used to apply rotations and forces to the hip while measuring torques and translations. An auxiliary motion capture system (Optotrak Certus™, NDI, Ontario, Canada) was used to track rigid arrays of infrared emitting diodes on the pelvis and femur to capture 6 degree of freedom hip kinematics. See previous study for a detailed description of methodology.

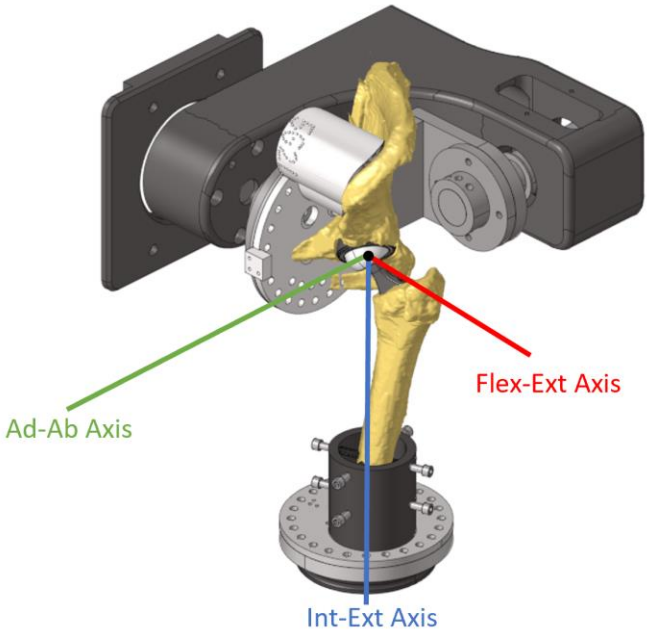

Figure 4.1: Hip Mounted in the AMTI VIVO 6 DOF Actuator with Labeled Rotational Axes

Experimental Testing:

One movement likely to cause an anterior dislocation and one movement likely to cause a posterior dislocation were each performed under four conditions: sutures intact and removed, to calculate the relative contribution of the capsular repair, and skeletonized with DM- and c-THA, to compare implant characteristics. The movement likely to result in an anterior dislocation hyperextended the hip from 0° to 30°, coupled with 0° of adduction-adduction and 1° of external rotation per degree of hyperextension (Fig. 4.2a). The movement likely to result in a posterior dislocation flexed the hip from 90° to 120°, coupled with 0.5° of adduction and 1° of internal rotation per degree of flexion (Fig. 4.2b). A 50 N compressive load and a 10 N medial load were applied to the hip via the femur to keep the implants in contact while the anterior-posterior load was set to 0 N.

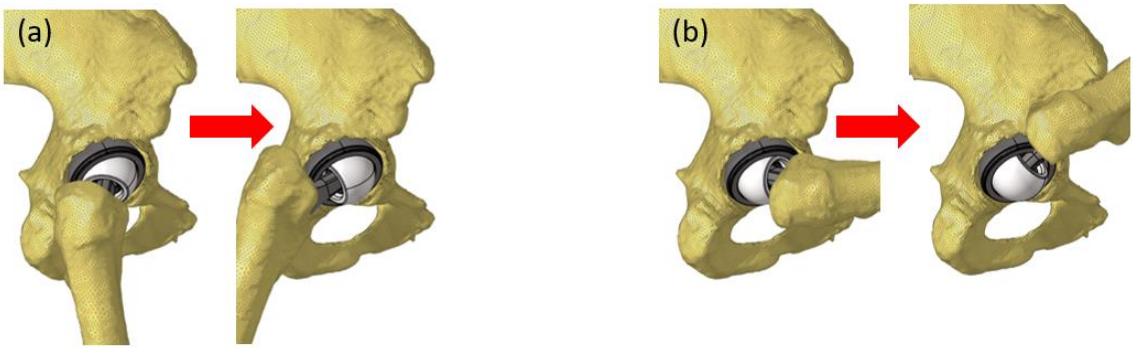

Figure 4.2: (a) Movement Likely to Cause Anterior Dislocations (b) Movement Likely to Cause Posterior Dislocations

When all DM-THA trials were complete (i.e., sutures intact, sutures removed, skeletonized), fiducial markers were implanted and digitized, and the femur and pelvis were white-light scanned with a Space Spider 3D Scanner (Artec, Luxembourg City, Luxembourg). Following the scans, the modular dual mobility liner was replaced with a c-THA PINNACLE® liner with an inner diameter of 28mm and an outer diameter to

match the acetabular shell (Depuy-Synthes, Warsaw, IN). The dual mobility head and articulating polyethylene liner were replaced with a 28mm femoral head with an offset of either +1.5mm, +5mm, or +8.5mm. The offset was chosen to best match the original DM-THA offset. The simulations were re-run and the pelvis and femur with c-THA components were white-light scanned again.

Post-Processing

The white-light scans of the skeletonized DM- and c-THA femur and pelvis were converted into 3D models and aligned to the original CT 3D models which defines neutral rotation and translation. Kinematics were calculated using data from the auxiliary motion capture system while forces and torques were recorded with the VIVO load-cell mounted below the femur. The VIVO data and kinematic data were synchronized to temporally align the data.

Torque-rotation curves were plotted for each trial and used to calculate various metrics of dislocation resistance. Torque was calculated as the sum of squared torques about all three axes and rotation was calculated as rotation about the medial-lateral axis (i.e., flexion/hyperextension). For the soft tissue trials (i.e., sutures intact and sutures removed), a least squares regression was performed on the linear region of the torque-rotation curve with the slope representing the stiffness and the transition to the linear region representing the passive tissue range of motion (Fig. 4.3a). For the skeletonized trials (i.e., DM- and c-THA), the impingement angle and torque were calculated as the abrupt change in torque and maximum torque, respectively (Fig. 4.3b). Additionally, the torque-rotation curve was integrated over the full trial to calculate the resistive energy during head egress.

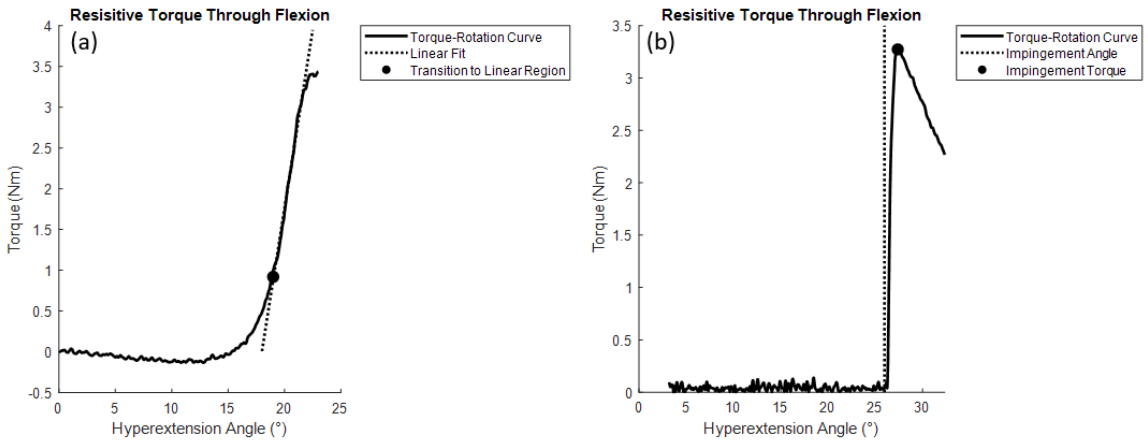

Figure 4.3: (a) Soft Tissue Torque-Rotation Curve (b) Skeletonized Torque-Rotation Curve

The impingement conditions for the skeletonized trials were observed during testing and verified using a custom MATLAB script which animated the experimental trials using the white-light scans and kinematic data. Component-component impingement was defined as contact between the femoral stem and acetabular liner, component-bone impingement was defined as contact between the femoral stem and osseous acetabulum, and bone-bone impingement was defined as contact between the femur and pelvis.

Statistical Analysis

A 2-way repeated measures analysis of variance (ANOVA) with a Tukey's post-hoc test was used to test for statistically significant differences between the sutures intact and sutures removed trials. Surgical approach (i.e., DAA/PA) and condition (i.e., sutures intact/removed) were used as the independent variables for the stiffness and passive range of motion analyses. A paired student t-test was run to determine statistically significant differences between the skeletonized trials. Implant type was used as the independent variable for the impingement angle, torque, and energy analyses. The significance level was set at $p < 0.05$.

4.3 Results

Surgical Technique Effects:

No statistically significant differences in stiffness were observed between the DAA and PA cohorts during movements likely to cause an anterior dislocation (Table 4.1). While not statistically significant, the mean stiffness was 0.54 Nm/° (186%) larger for PA than DAA, for both the sutures intact and removed cases. The passive range of motion was significantly larger for DAA ($p = 0.001$) than PA. The mean increase in range of motion for the DAA specimens was 17.7° with sutures intact ($p < 0.001$) and 17.2° with sutures removed ($p = .014$).

Table 4.1: Results from Sutures Intact/Removed Hyperextension Trials

	Anterior Approach n=5 (Sutures Intact)	**Anterior Approach n=5 (Sutures Removed)**	**Posterior Approach n=5 (Sutures Intact)**	**Posterior Approach n=5 (Sutures Removed)**
Stiffness	0.63 ± 0.25 Nm/°	0.63 ± 0.19 Nm/°	1.17 ± 0.59 Nm/°	1.17 ± 0.60 Nm/°
Passive Tissue Range of Motion	19.3 ± 3.8°	19.7 ± 4.5°	1.6 ± 0.6°	2.5 ± 5.7°

No statistically significant differences in stiffness were observed between the DAA and PA cohorts during movements likely to cause a posterior dislocation (Table 4.2). While not statistically significant, the mean stiffness was 0.75 Nm/° (195%) larger for the PA specimens with sutures than without. Additionally, there was a non-significant increase in passive range of motion for the PA specimens of 8.9° with sutures intact and 4.0° with sutures removed.

Table 4.2: Results from Sutures Intact/Removed Flexion Trials

	Anterior Approach n=5 (Sutures Intact)	**Anterior Approach n=5 (Sutures Removed)**	**Posterior Approach n=5 (Sutures Intact)**	**Posterior Approach n=5 (Sutures Removed)**
Stiffness	1.45 ± 1.44 Nm/°	1.27 ± 0.84 Nm/°	1.55 ± 0.50 Nm/°	0.79 ± 0.68 Nm/°
Passive Tissue Range of Motion	93.0 ± 4.4°	97.0 ± 7.0°	101.9 ± 6.0°	101.0 ± 5.9°

Implant Effects:

6 of the 10 hips impinged during the movements likely to cause an anterior dislocation with component-component impingement being the most common impingement type (Table 4.3). No significant difference was found between the two implant types for impingement free range of motion ($p = 0.496$) or resistive energy ($p = 0.080$), however, the DM-THA components provided significantly more resistive torque than the c-THA components ($p = 0.036$). The statistical calculations and the values reported in Table 4.3 only included the 6 specimens which impinged.

Table 4.3: Results from Skeletonized DM- and c-THA Hyperextension Trials

	DM-THA n=10	**c-THA n=10**
Impingement Type	Component-Component n=4 Bone-Bone n=2 No Impingement n=4	Component-Component n=4 Bone-Bone n=2 No Impingement n=4
Impingement Angle	$24.2 \pm 4.8^\circ$	$24.9 \pm 6.1^\circ$
Resistive Torque	1.91 ± 1.04 Nm	1.12 ± 0.42 Nm
Resistive Energy	15.60 ± 16.85 Nm·°	9.34 ± 10.66 Nm·°

All 10 hips impinged during the movements likely to cause a posterior dislocation with component-component being the most common dislocation condition (Table 4.4). Component-component impingement occurred between the femoral stem and the superior aspect of the liner, component-bone impingement occurred between the femoral stem and superior aspect of the osseous acetabulum, and bone-bone impingement occurred between the femur and superior aspect of the osseous acetabulum. No significant difference was found between the two implant types for impingement free range of motion ($p = 0.439$), however, the DM-THA components had significantly larger resistive torques ($p < 0.001$) and resistive energy ($p = 0.013$).

Table 4.4: Results from Skeletonized DM- and c-THA Flexion Trials

	DM-THA n=10	**c-THA n=10**
Impingement Type	Component-Component n=5 Component-Bone n=4 Bone-Bone n=1	Component-Component n=5 Component-Bone n=4 Bone-Bone n=1
Impingement Angle	100.4 ± 7.6°	99.8 ± 6.4°
Resistive Torque	1.44 ± 0.63 Nm	1.08 ± 0.59 Nm
Resistive Energy	19.77 ± 6.53 Nm·°	16.25 ± 6.57 Nm·°

4.4 Discussion

The repeated measures design of this study allowed for comparisons of surgical approach and effects of capsular repair during motions likely to cause anterior and posterior dislocations. Additionally, the modular implants allowed for DM- and c-THA implants to be swapped to compare impingement free ROM and mechanics of impingement between the two designs.

The results from this study suggest that the PA provides more stability in resisting anterior dislocations. During the combined hyperextension and external rotation, the soft tissue structures became taut significantly sooner for the PA specimens than the DAA specimens. This supports a previous finding that in extended positions, the anterior capsulotomy had a greater passive tissue range of motion (Lgoishetty et al., 2019). This is beneficial as it limits range of motion and may prevent the hip from impinging and dislocating.

The sutures had relatively small effects on both the stiffness and passive tissue range of motion, except for the PA specimens during movements likely to induce a posterior dislocation. While the differences were not statistically different, the capsular repair was on average, nearly twice as stiff than no repair. Similar studies have found that a posterior repair provided more torque during a motion likely to cause a posterior

dislocation (e.g., flexion and internal rotation) but their results were also not statistically different. (Mihalko and Whiteside, 2004; Sioen et al., 2002). However, both studies found that significantly more torque is required to dislocate a hip following transosseous repair than soft tissue repair alone, which highlights the potential benefit of this technique.

When calculating the stiffness and passive tissue ROM metrics for the sutures intact and removed trials, the torque-rotation curve did not always display a defined toe-in region and transition to linear region. Some specimens already had a taut capsule (i.e., already in the linear range) which resulted in an overestimation of the passive tissue range. Additionally, as some specimens impinged within the hyperextension/flexion range, the torque-rotation curve had a sudden change in measured torque which affected the accuracy of the linear fit.

The skeletonized trials provided useful insight into the different modes of impingement; however, soft-tissue impingement was also seen in multiple cases. Using the translational kinematics, the head was found to egress sooner in the soft tissue cases than the skeletonized cases during 50% of motions likely to cause posterior dislocations and 40% of motions likely during to cause anterior dislocations. This further decreased the impingement free range of motion and suggests that the mean impingement free ROM reported for the skeletonized hips would be smaller for living subjects. It is hypothesized that this iliopsoas impingement, as this is a common complication in patients following THA and can be caused by a protruded acetabular component (Dora et al., 2007).

While previous studies have reported an increased impingement free ROM with DM-THA (Guyen et al., 2007), our results showed statistically insignificant differences. The main difference between the two studies was that Guyen et al., used an anatomically designed shell while our study used a modular shell. As the modular dual mobility implant we used has an additional liner with a 3 mm cylindrical extension, the impingement free ROM was theoretically decreased. However, while impingement free range of motion decreases with the cylindrical extension, jump distance increases which provides additional dislocation resistance.

When comparing torques between the two implants, it was found DM-THA provided significantly more resistive torque than c-THA. This is contradictory to previous findings which showed that DM-THA decreased resistive torque (Klemt et al., 2020; Terrier et al., 2017). These differences may be due to their use of monoblock dual mobility shell and our use of modular dual mobility. It was found that the constrained tripolar implant in their studies provided a greater resistive torque than DM-THA, which may behave similarly to modular dual mobility since both utilize a secondary liner on the acetabular side

A secondary finding was that impingement on the osseous pelvis (i.e., component-bone and bone-bone impingement) significantly increased the resistive torque during both the hyperextension and flexion trials when compared to impingement on the liner (i.e., component-component) ($p < 0.05$, 2 sample t-test). For both movements likely to cause anterior and posterior dislocations, the mean increase in torque was more than twice as large when osseous impingement occurred. We hypothesize that this is due to a larger moment arm on the impingement side since the distance from the head center is

further to the osseous pelvis than to the edge of the liner. Previous studies have shown that larger heads are likely to result in bone-bone impingement (Bartz et al., 2000; Burroughs et al., 2005), which would subsequently increase the resistive torque based on our findings.

The resistive torques reported in this study should be viewed with caution due to the boundary conditions applied. A 50 N superior load and 10 N medial load were applied to the hip via the femur with the sole intent of keeping the implant seated through the simulations. However, some dislocation prone maneuvers such as rolling over in bed may have smaller compressive loads while other maneuvers such as pivoting may have higher compressive loads.

During the movement likely to cause a posterior dislocation, the differences in resistive energy were significantly larger for the DM-THA, however, no statistically significant differences were found during the motions likely to cause an anterior dislocation. Due to mechanical limits on the actuator, some specimens impinge at the end of the torque-rotation curve and have a small area under the curve while other specimens impinge at the start of the torque-rotation curve and have a large area under the curve. We hypothesize that if all specimens rotated to dislocation, DM-THA would require more energy to dislocate because the resistive torque is greater than c-THA, and the increase in jump distance would require more rotation.

While this study provides useful insight into impingement mechanics, there were a few limitations. Along with a small sample size, all surgeries were performed by different orthopaedic surgeons using their own surgical technique and choice of implant/sizing, therefore, a large variance was seen across the specimens. Additionally,

as the outer diameter of some implanted DM-THA femoral heads was 22.225 mm while all c-THA femoral heads were 28 mm, there was not always a direct match in offset choice. However, the difference in offset between DM- and c-THA was always ≤ 1.5 mm.

The results from this study highlight a few clinically relevant findings. The findings support the use of dual-mobility (or potentially c-THA with a large femoral head) as they provide a larger resistive torque upon impingement, which may reduce the risk of subluxation and dislocation. Furthermore, larger femoral heads will increase the jump distance and require more rotation to dislocation. Additionally, knowing that the PA provides more stability in resisting anterior dislocations could potentially factor into pre-operative surgical plans.

CHAPTER 5: Conclusion

5.1 Main Findings

The work presented in Chapter 3 highlights how various factors affect range of motion during internal and external rotations through flexion. It was found that through flexion, impingement free range of motion decreased for internal rotation and increased for external rotation. At full extension, the anterior approach specimens were more likely to impinge during external rotation prior to soft tissue structures becoming taut. Conversely, in deep flexion, the posterior approach specimens were more likely to impinge during internal rotation prior to soft tissue structures becoming taut.

The work presented in Chapter 4 highlights how surgical approach, technique, and implant selection affect dislocation resistance. The results suggest that the posterior approach provides more resistance to anterior dislocations by becoming taut sooner in the rotation. Capsular repair was most effective for the posterior approach specimens during combined flexion, adduction, and internal rotation; however, the differences were not significant at the $p < 0.05$ level. In skeletonized hips, dual mobility implants provided significantly more resistive torque than the conventional implants, and bony impingement on the pelvis provided significantly more torque than impingement on the acetabular liner.

5.2 Future Work

To expand on the research presented in the two studies, the experimental results from this study will be used to calibrate finite element based capsule models. Using these subject specific models, the effect of surgical approach, capsular repair and implant design on dislocation mechanics can be studied. While studying surgical approach, the finite element models can provide insight into which aspects of the capsule are loaded during the movements likely to induce anterior and posterior dislocations. These models will further be used to understand different capsular repair techniques. Finally, the models can be used to further analyze implant designs, specifically, the impingement behavior in dual mobility and conventional THA to understand their resistance to dislocation.

REFERENCES

Adam, P., Farizon, F., Fessy, M.H., 2014. Dual mobility retentive acetabular liners and wear: Surface analysis of 40 retrieved polyethylene implants. Orthopaedics and Traumatology: Surgery and Research. https://doi.org/10.1016/j.otsr.2013.12.011

Arac, S., Boya, H., Ozcan, O., Oztekin, H.H., 2006. Anterior Capsular Repair in Total Hip Arthroplasty Performed for Late-Presenting Displaced Femoral Neck Fractures. Hip International 16, 198–201.

Bartz, R.L.;, Noble, P.C.;, Kadakia, N.R.;, Tullios, H.S., 2000. The effect of femoral component head size on posterior dislocation of the artificial hip joint, Journal of Bone and Joint Surgery.

Blakeney, W.G., Epinette, J.A., Vendittoli, P.A., 2019. Dual mobility total hip arthroplasty: Should everyone get one? EFORT Open Reviews 4, 541–547. https://doi.org/10.1302/2058-5241.4.180045

Bourne, R.B., Mehin, R., 2004. The dislocating hip: What to do, what to do, in: Journal of Arthroplasty. pp. 111–114. https://doi.org/10.1016/j.arth.2004.02.016

Brown, T.D., Elkins, J.M., Pedersen, D.R., Callaghan, J.J., 2014. IMPINGEMENT AND DISLOCATION IN TOTAL HIP ARTHROPLASTY: MECHANISMS AND CONSEQUENCES. The Iowa Orthopaedic Journal 34, 1–15.

Brun, O.-C., Månsoon, L., Nordsletten, L., 2018. The direct anterior minimal invasive approach in total hip replacement: a prospective departmental study on the learning curve. HIP International 28, 156–160.

Burroughs, B.R., Hallstrom, B., Golladay, G.J., Hoeffel, D., Harris, W.H., 2005. Range of motion and stability in total hip arthroplasty with 28-, 32-, 38-, and 44-mm femoral head sizes: An in vitro study. Journal of Arthroplasty 20, 11–19. https://doi.org/10.1016/j.arth.2004.07.008

Dawson-Amoah, K., Raszewski, J., Duplantier, N., Waddell, B.S., 2018. Dislocation of the Hip: A Review of Types, Causes, and Treatment. Ochsner Journal 18, 242–252. https://doi.org/10.31486/toj.17.0079

de Martino, I., Triantafyllopoulos, G.K., Sculco, P.K., Sculco, T.P., 2014. Dual mobility cups in total hip arthroplasty. World Journal of Orthopaedics 5, 180–187. https://doi.org/10.5312/wjo.v5.i3.180

D'lima, D.D., Urquhart, A.G., Buehler, K.O., Walker, R.H., Colwell, C.W., 2000. The Effect of the Orientation of the Acetabular and Femoral Components on the Range of Motion of the Hip at Different Head-Neck Ratios. The Journal of Bone and Joint Surgery 82-A, 315–321.

Dora, C., Houweling, M., Koch, P., Sierra, R.J., 2007. Iliopsoas impingement after total hip replacement THE RESULTS OF NON-OPERATIVE MANAGEMENT, TENOTOMY OR ACETABULAR REVISION. J Bone Joint Surg [Br] 89, 1031–1036. https://doi.org/10.1302/0301-620X.89B8

Dorr, L.D., 2014. Dislocation, in: Successful Techniques for Total Hip Replacement. Future Medicine Ltd., pp. 105–118. https://doi.org/10.2217/FMEB2013.13.203

Dowsey, M.M., Nikpour, M., Dieppe, P., Choong, P.F.M., 2016. Associations between pre-operative radiographic osteoarthritis severity and pain and function after total hip replacement: Radiographic osteoarthritis severity predicts function after total hip replacement. Clinical Rheumatology 35, 183–189. https://doi.org/10.1007/s10067-014-2808-7

Elkins, J.M., Daniel, M., Pedersen, D.R., Singh, B., Yack, H.J., Callaghan, J.J., Brown, T.D., 2013. Morbid obesity may increase dislocation in total hip patients: A biomechanical Analysis Hip. Clinical Orthopaedics and Related Research 471, 971–980. https://doi.org/10.1007/s11999-012-2512-3

Elkins, J.M., Stroud, N.J., Rudert, M.J., Tochigi, Y., Pedersen, D.R., Ellis, B.J., Callaghan, J.J., Weiss, J.A., Brown, T.D., 2011. The Capsule's Contribution to Total Hip Construct Stability – A Finite Element Analysis. Journal of Orthopaedic Research 29, 1642–1648. https://doi.org/10.1002/jor.21435

Esposito, C.I., Gladnick, B.P., Lee, Y. yu, Lyman, S., Wright, T.M., Mayman, D.J., Padgett, D.E., 2015. Cup Position Alone Does Not Predict Risk of Dislocation After Hip Arthroplasty. The Journal of Arthroplasty 30, 109–113. https://doi.org/10.1016/j.arth.2014.07.009

Guyen, O., 2016. Constrained liners, dual mobility or large diameter heads to avoid dislocation in THA. EFORT Open Rev 1, 197–204. https://doi.org/10.1302/2058-5241.1.000054

Guyen, O., Chen, Q.S., Bejui-Hugues, J., Berry, D.J., An, K.N., 2007. Unconstrained Tripolar Hip Implants: Effect on Hip Stability. Clinical Orthopaedics and Related Research 455, 202–208. https://doi.org/10.1097/01.blo.0000238796.59596.1f

Guyen, O., Pibarot, V., Vaz, G., Chevillotte, C., Béjui-Hugues, J., 2009. Use of a dual mobility socket to manage total hip arthroplasty instability. Clinical Orthopaedics and Related Research 467, 465–472. https://doi.org/10.1007/s11999-008-0476-0

Han, S., Owens, V.L., Patel, R. v., Ismaily, S.K., Harrington, M.A., Incavo, S.J., Noble, P.C., 2020. The continuum of hip range of motion: From soft-tissue restriction to bony impingement. Journal of Orthopaedic Research 38, 1779–1786. https://doi.org/10.1002/jor.24594

Higgins, B.T., Barlow, D.R., Heagerty, N.E., Lin, T.J., 2015. Anterior vs. Posterior Approach for Total Hip Arthroplasty, a Systematic Review and Meta-analysis. Journal of Arthroplasty 30, 419–434. https://doi.org/10.1016/j.arth.2014.10.020

Incavo, S.J., Thompson, M.T., Gold, J.E., Patel, R. v., Icenogle, K.D., Noble, P.C., 2011. Which Procedure Better Restores Intact Hip Range of Motion: Total Hip Arthroplasty or Resurfacing? A Combined Cadaveric and Computer Simulation Study. Journal of Arthroplasty 26, 391–397. https://doi.org/10.1016/j.arth.2010.02.001

Jurkutat, J., Zajonz, D., Sommer, G., Schleifenbaum, S., Möbius, R., Grunert, R., Hammer, N., Prietzel, T., 2018. The impact of capsular repair on the risk for dislocation after revision total hip arthroplasty - A retrospective cohort-study of 259 cases. BMC Musculoskeletal Disorders 19. https://doi.org/10.1186/s12891-018-2242-0

Kessler, O., Patil, S., Stefan, W., Mayr, E., Colwell, C.W., D'Lima, D.D., 2008. Bony Impingement Affects Range of Motion after Total Hip Arthroplasty: A Subject-Specific Approach. Journal of Orthopaedic Research 26, 443–452. https://doi.org/10.1002/jor.20541

Klemt, C., Bounajem, G., Tirumala, V., Liang Xiong, |, 2020. Three-dimensional kinematic analysis of dislocation mechanism in dual mobility total hip arthroplasty constructs. Journal of Orthopaedic Research 1–10. https://doi.org/10.1002/jor.24855

Kluess, D., Martin, H., Mittelmeier, W., Schmitz, K.P., Bader, R., 2007. Influence of femoral head size on impingement, dislocation and stress distribution in total hip replacement. Medical Engineering and Physics 29, 465–471. https://doi.org/10.1016/j.medengphy.2006.07.001

Kunutsor, S.K., Barrett, M.C., Beswick, A.D., Judge, A., Blom, A.W., Wylde, V., Whitehouse, M.R., 2019. Risk factors for dislocation after primary total hip replacement: a systematic review and meta-analysis of 125 studies involving approximately five million hip replacements. The Lancet Rheumatology 1, e111–e121. https://doi.org/10.1016/S2665-9913(19)30045-1

Kwon, M.S., Kuskowski, M., Mulhall, K.J., Macaulay, W., Brown, T.E., Saleh, K.J., 2006. Does Surgical Approach Affect Total Hip Arthroplasty Dislocation Rates? Clinical Orthopaedics and Related Research 447, 34–38. https://doi.org/10.1097/01.blo.0000218746.84494.df

Leunig, M., Ganz, R., 2014. The evolution and concepts of joint-preserving surgery of the hip. The Bone & Joint Journal 96-B, 5–18. https://doi.org/10.1302/0301-620X.96B1

Lewinnek, G.E., Lewis, J.L., Tarr, R., Compere, C.L., Zimmerman, J.R., 1978. Dislocations after total hip-replacement arthroplasties. The Journal of Bone and Joint Surgery 60-A, 217–220.

Lgoishetty, K., van Arkel, R.J., Ng, K.C.G., Muirhead-Allwood, S.K., Cobb, J.P., Jeffers, J.R.T., 2019. Hip capsule biomechanics after arthroplasty: THE EFFECT OF IMPLANT, APPROACH, AND SURGICAL REPAIR. Bone and Joint Journal 101-B, 426–434. https://doi.org/10.1302/0301-620X.101B4

Maldonado, D.R., Kyin, C., Walker-Santiago, R., Rosinsky, P.J., Shapira, J., Lall, A.C., Domb, B.G., 2019. Direct anterior approach versus posterior approach in primary total hip replacement: comparison of minimum 2-year outcomes. HIP International 31, 166–173. https://doi.org/10.1177/1120700019881937

Malek, I.A., Royce, G., Bhatti, S.U., Whittaker, J.P., Phillips, S.P., Wilson, I.R.B., Wootton, J.R., Starks, I., 2016. A comparison between the direct anterior and posterior approaches for total hip arthroplasty: THE ROLE OF AN 'ENHANCED RECOVERY' PATHWAY. The Bone and Joint Journal 98-B, 754–760. https://doi.org/10.1302/0301-620X.98B6

Maratt, J.D., Gagnier, J.J., Butler, P.D., Hallstrom, B.R., Urquhart, A.G., Roberts, K.C., 2016. No Difference in Dislocation Seen in Anterior Vs Posterior Approach Total Hip Arthroplasty. The Journal of Arthroplasty 31, S127–S130. https://doi.org/10.1016/j.arth.2016.02.071

Masonis, J., Bourne, R., 2002. Masonis et al., 2002-Surgical Approach, Abductor Function, and Total Hip Arthroplasty Dislocation. Clinical Orthopeadics and Related Research 405, 46–53.

Matsen Ko, L.J., Pollag, K.E., Yoo, J.Y., Sharkey, P.F., 2016. Serum Metal Ion Levels Following Total Hip Arthroplasty With Modular Dual Mobility Components. Journal of Arthroplasty 31, 186–189. https://doi.org/10.1016/j.arth.2015.07.035

Matta, J., Ferguson, T., 2005. Matta et al., 2005-The Anterior Approach for Hip Replacement. Orthopedics 28, 927–928.

Mihalko, W.M., Whiteside, L.A., 2004. Hip Mechanics After Posterior Structure Repair in Total Hip Arthroplasty. Clinical Orthopaedics and Related Research 420, 194–198. https://doi.org/10.1097/01.blo.0000126221.38764.cc

Miller, L.E., Gondusky, J.S., Kamath, A.F., Boettner, F., Wright, J., Bhattacharyya, S., 2018. Influence of surgical approach on complication risk in primary total hip arthroplasty: Systematic review and meta-analysis. Acta Orthopaedica 89, 289–294. https://doi.org/10.1080/17453674.2018.1438694

Möller, T., Trumbore, B., 1997. Fast, Minimum Storage Ray & Triangle Intersection. Journal of Graphics Tools 2, 21–28.

Nadzadi, M.E., Pedersen, D.R., Yack, H.J., Callaghan, J.J., Brown, T.D., 2003. Kinematics, kinetics, and finite element analysis of commonplace maneuvers at risk for total hip dislocation. Journal of Biomechanics 36, 577–591.

Nakahara, I., Takao, M., Sakai, T., Nishii, T., Yoshikawa, H., Sugano, N., 2011. Gender differences in 3D morphology and bony impingement of human hips. Journal of Orthopaedic Research 29, 333–339. https://doi.org/10.1002/jor.21265

Palit, A., King, R., Hart, Z., Gu, Y., Pierrepont, J., Elliott, M.T., Williams, M.A., 2020. Bone-to-Bone and Implant-to-Bone Impingement: A Novel Graphical Representation for Hip Replacement Planning. Annals of Biomedical Engineering 48, 1354–1367. https://doi.org/10.1007/s10439-020-02451-x

Pedersen, D.R., Callaghan, J.J., Brown, T.D., 2005. Activity-dependence of the "safe zone" for impingement versus dislocation avoidance. Medical Engineering and Physics 27, 323–328. https://doi.org/10.1016/j.medengphy.2004.09.004

Pfirrmann, C.W.A., Mengiardi, B., Dora, C., Kalberer, F., Zanetti, M., Hodler, J., 2006. Cam and Pincer Femoroacetabular Impingement: Characteristic MF Arthrographic Findings in 50 Patients. Radiology 240, 778–785. https://doi.org/10.1148/radiol.2403050767

Philippot, R., Boyer, B., Farizon, F., 2013. Intraprosthetic dislocation: A specific complication of the dual-mobility system hip. Clinical Orthopaedics and Related Research 471, 965–970. https://doi.org/10.1007/s11999-012-2639-2

Sariali, E., Lazennec, J.Y., Khiami, F., Catonné, Y., 2009. Mathematical evaluation of jumping distance in total hip arthroplasty: Influence of abduction angle, femoral head offset, and head diameter. Acta Orthopaedica 80, 277–282. https://doi.org/10.3109/17453670902988378

Scifert, C.F., Brown, T.D., Lipman, J.D., 1999. Finite element analysis of a novel design approach to resisting total hip dislocation. Clinical Biomechanics 14, 697–703.

Scifert, C.F., Noble, P.C., Brown, T.D., Bartz, R.L., Kadakia, N., Sugano, N., Johnston, R.C., Pedersen, D.R., Callaghan, J.J., 2001. Experimental and computational simulation of total hip arthroplasty dislocation. Orthopedic Clinics of North America 32, 553–567. https://doi.org/10.1016/S0030-5898(05)70226-1

Siguier, T., Siguier, M., Brumpt, B., 2004. Mini-incision anterior approach does not increase dislocation rate: A study of 1037 total hip replacements. Clinical Orthopaedics and Related Research 164–173. https://doi.org/10.1097/01.blo.0000136651.21191.9f

Singh, J.A., Yu, S., Chen, L., Cleveland, J.D., 2019. Rates of total joint replacement in the United States: Future projections to 2020-2040 using the national inpatient sample. Journal of Rheumatology 46, 1134–1140. https://doi.org/10.3899/jrheum.170990

Sioen, W., Simon, J.P., Labey, L., R Van Audekercke, 2002. POSTERIOR TRANSOSSEOUS CAPSULOTENDINOUS REPAIR IN TOTAL HIP ARTHROPLASTY?: A CADAVER STUDY. Journal of Bone and Joint Surgery 84, 1763–1798.

Siopack, J., Jergesen, H., 1995. Total Hip Arthroplasty. Western Journal of Medicine 162, 243–249.

Steiger, R.N., Lorimer, M., Solomon, M., 2015. What Is the Learning Curve for the Anterior Approach for Total Hip Arthroplasty. Clinical Orthopaedics and Related Research 473, 3860–3866.

Sutter, E.G., McClellan, T.R., Attarian, D.E., Bolognesi, M.P., Lachiewicz, P.F., Wellman, S.S., 2017. Outcomes of Modular Dual Mobility Acetabular Components in Revision Total Hip Arthroplasty. Journal of Arthroplasty 32, S220–S224. https://doi.org/10.1016/j.arth.2017.03.035

Swanson, T. v., Kukreja, M.M., Ballard, J.C., Calleja, H.G.M., Brown, J.M., 2019. The "capsular noose": A new capsular repair technique to diminish dislocation risk after the posterior approach total hip arthroplasty. International Journal of Surgery Open 17, 8–14. https://doi.org/10.1016/j.ijso.2018.12.005

Tannast, M., Hanke, M., Ecker, T.M., Murphy, S.B., Albers, C.E., Puls, M., 2012. LCPD: Reduced Range of Motion Resulting From Extra- and Intraarticular Impingement. Clinical Orthopaedics and Related Research 470, 2431–2440. https://doi.org/10.1007/s11999-012-2344-1

Tannast, M., Kubiak-Langer, M., Langlotz, F., Puls, M., Murphy, S.B., Siebenrock, K.A., 2007. Noninvasive three-dimensional assessment of femoroacetabular impingement. Journal of Orthopaedic Research 25, 122–131. https://doi.org/10.1002/jor.20309

Tay, K., Tang, A., Fary, C., Patten, S., Steele, R., de Steiger, R., 2019. The effect of surgical approach on early complications of total hip arthoplasty. Arthroplasty 1. https://doi.org/10.1186/s42836-019-0008-2

Terrier, A., Latypova, A., Guillemin, M., Parvex, V., Guyen, O., 2017. Dual mobility cups provide biomechanical advantages in situations at risk for dislocation: a finite element analysis. International Orthopaedics 41, 551–556. https://doi.org/10.1007/s00264-016-3368-z

van Arkel, R., Ng, G., Muirhead-Allwood, S., Jeffers, J., 2018. van Arkel et al., 2018-Capsular Ligament Function After Total Hip Arthroplasty.

van Arkel, R.J., Amis, A.A., Jeffers, J.R.T., 2015. The envelope of passive motion allowed by the capsular ligaments of the hip. Journal of Biomechanics 48, 3803–3809. https://doi.org/10.1016/j.jbiomech.2015.09.002

Waddell, J., Johnson, K., Hein, W., Raabe, J., FitzGerald, G., Turibio, F., 2010. Orthopedic Practice in Total Hip and Total Knee Arthroplasty Results From the Global Orthopaedic Registry (GLORY). American Journal of Orthopedics 39, 5–13.

White, R., Forness, T., Allman, J., Junick, D., 2001. Effect of Posterior Capsular Repair on Early Dislocation in Primary Total Hip Replacement. Clinical Orthopaedics and Related Research 393, 163–167.

Yerasimides, J.G., Matta, J.M., 2005. Primary total hip arthroplasty with a minimally invasive anterior approach. Seminars in Arthroplasty 16, 186–190. https://doi.org/10.1053/j.sart.2005.10.004

APPENDICES

Appendix A: Specimen Information

Table A.1: Specimen Information

Specimen	Approach	Stem Implant	Shell Implant	Dual Mobility Liner	Poly Head	Femoral Head	Acetabular Inclination	Acetabular Anteversion	Femoral Version
C191002L	Anterior	Corail KA Sz 14	Pinnacle Gription 58mm	58/49	SERF 49/28	28+1.5	40.4°	26.9°	35.9°
C191002R	Posterior	Summit Size 5 High Offset	Pinnacle Gription 60mm	60/51	SERF 51/28	28+1.5	51.5°	36.7°	41.2°
C191008L	Anterior	Corail KS Size 15 Std Offset	Pinnacle Gription 54mm	54/47	SERF 47/28	28 +8.5	52.9°	20.0°	4.3°
C191008R	Posterior	Corail KHO Size 14 High Offset	Pinnacle Gription 52mm	52/45	SERF 45/22.2	22.225+7	45.2°	25.0°	19.3°
L191562L	Anterior	Corail KS Size 12 Std Offset	Pinnacle Gription 50mm	50/43	SERF 43/22.2	22.225+7	43.6°	25.7°	19.5°
L191562R	Posterior	Summit Size 5 High Offset	Pinnacle Gription 50mm	50/43	SERF 43/22.2	22.225+4	47.5°	35.3°	29.7°
L191570L	Posterior	Summit Size 2 High Offset	Pinnacle Gription 54mm	54/47	SERF 47/28	28+8.5	46.7°	25.3°	20.1°
L191570R	Anterior	Corail KS Size 11 Std Offset	Pinnacle Gription 52mm	52/45	SERF 45/22.2	22.225+4	46.1°	26.8°	4.8°
S192577L	Anterior	Corail KS size 10 Std Offset	Pinnacle Gription 48mm	48/41	SERF 41/22.2	22.225+4	36.8°	27.6°	23.6°
S192577R	Posterior	Corail KS size 10 Std Offset	Pinnacle Gription 48mm	48/41	SERF 41/22.2	22.225+4	43.0°	20.6°	17.7°

Appendix B: Impingement Free ROM Plots

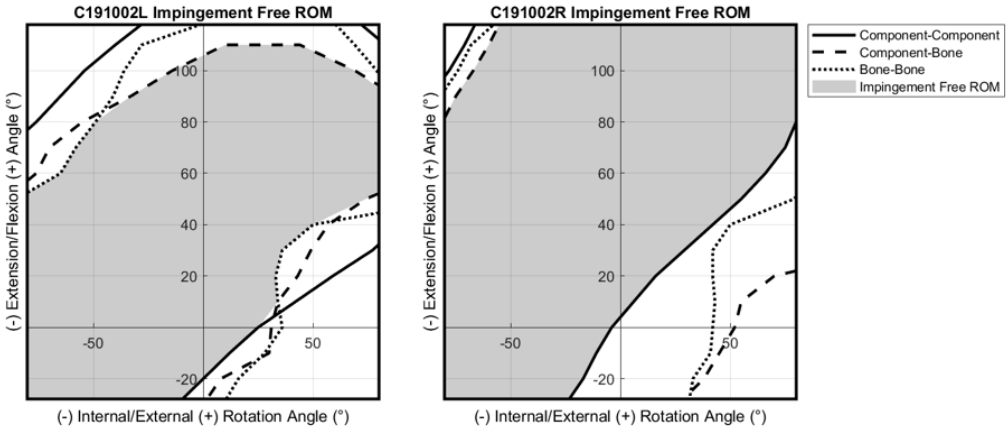

Figure B.1: Specimen C191002 Impingement Free ROM Contours

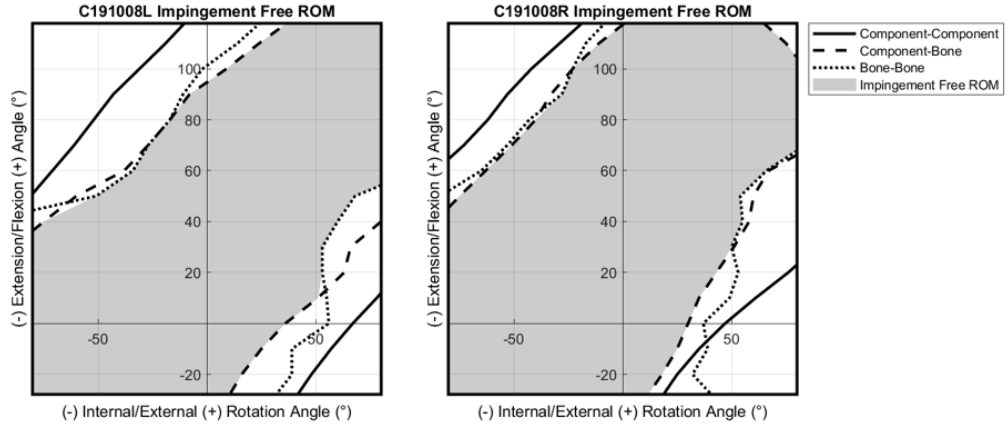

Figure B.2: Specimen C191008 Impingement Free ROM Contours

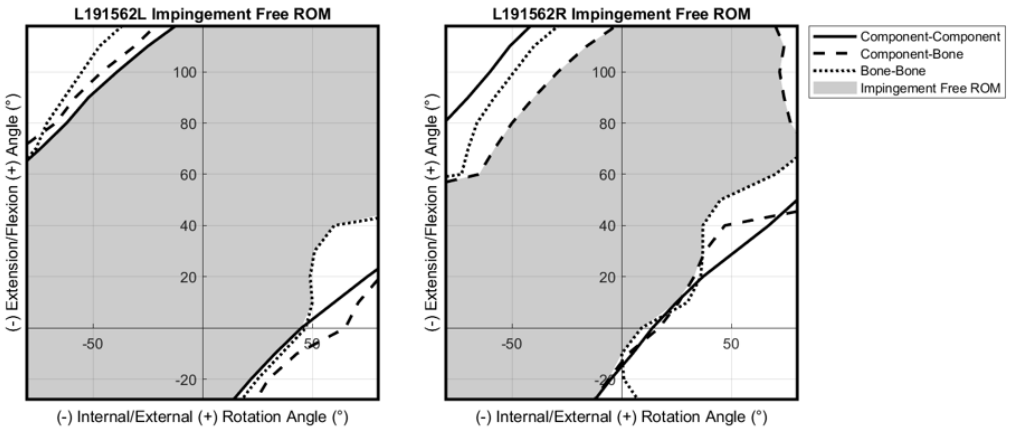

Figure B.3: Specimen L191562 Impingement Free ROM Contours

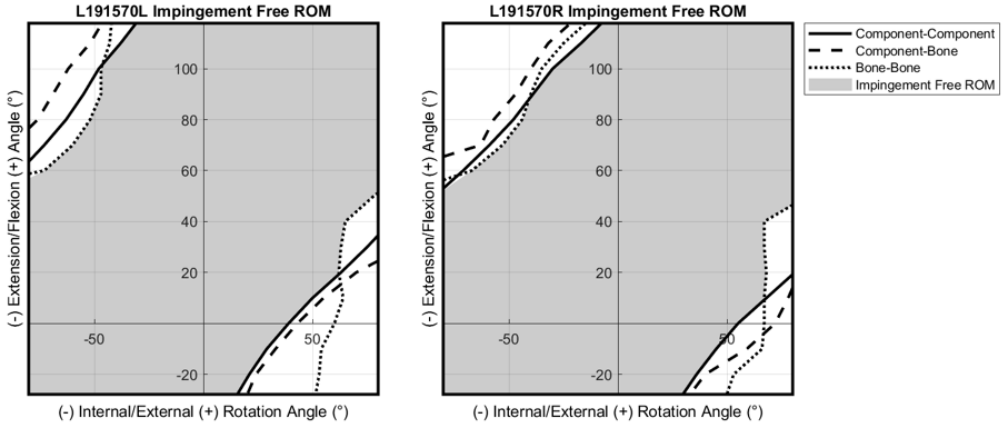

Figure B.4: Specimen L191570 Impingement Free ROM Contours

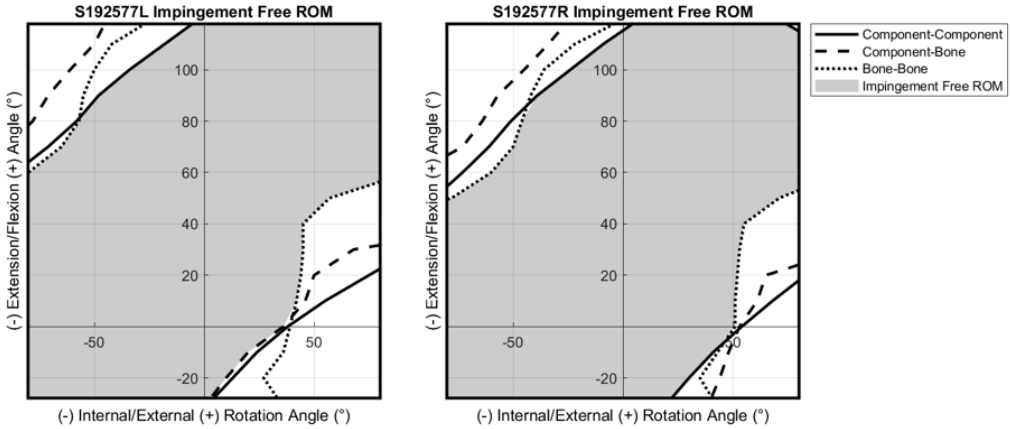

Figure B.5: Specimen S192577 Impingement Free ROM Contours

Appendix C: Sutures Intact & Sutures Removed Int-Ext Laxity Plots

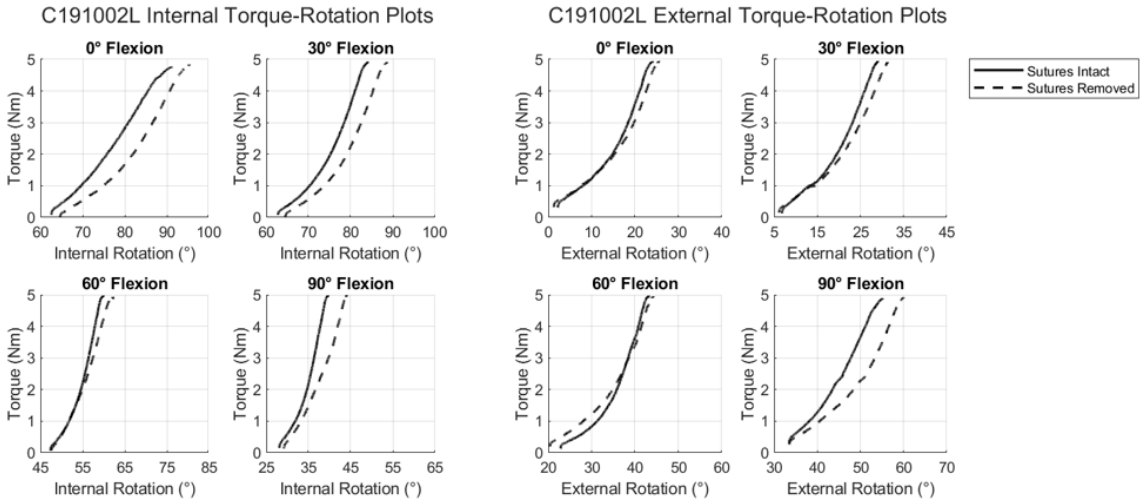

Figure C.1: Specimen C191002L Internal & External Torque-Rotation Curves at Various Flexion Angles

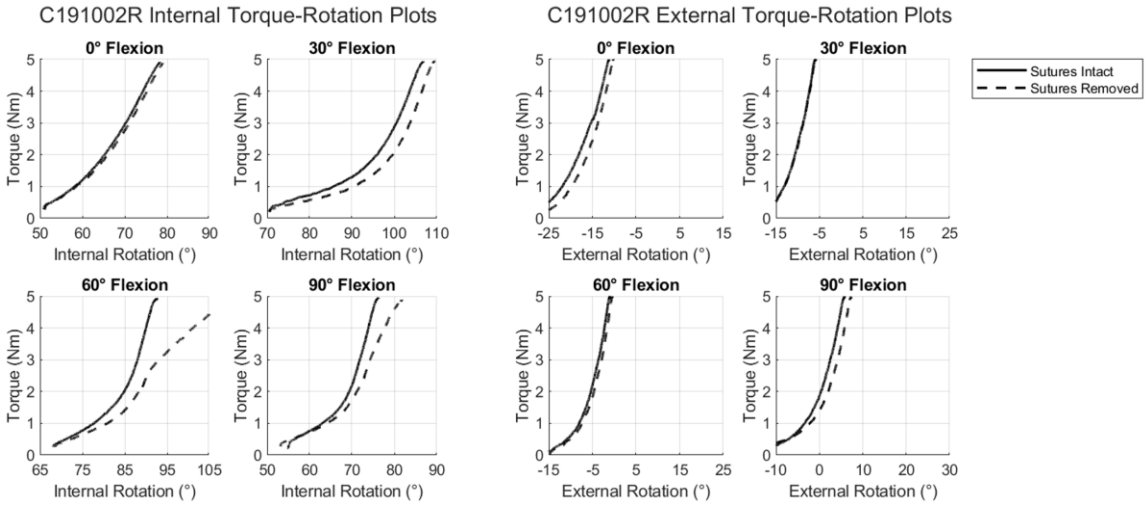

Figure C.2: Specimen C191002R Internal & External Torque-Rotation Curves at Various Flexion Angles

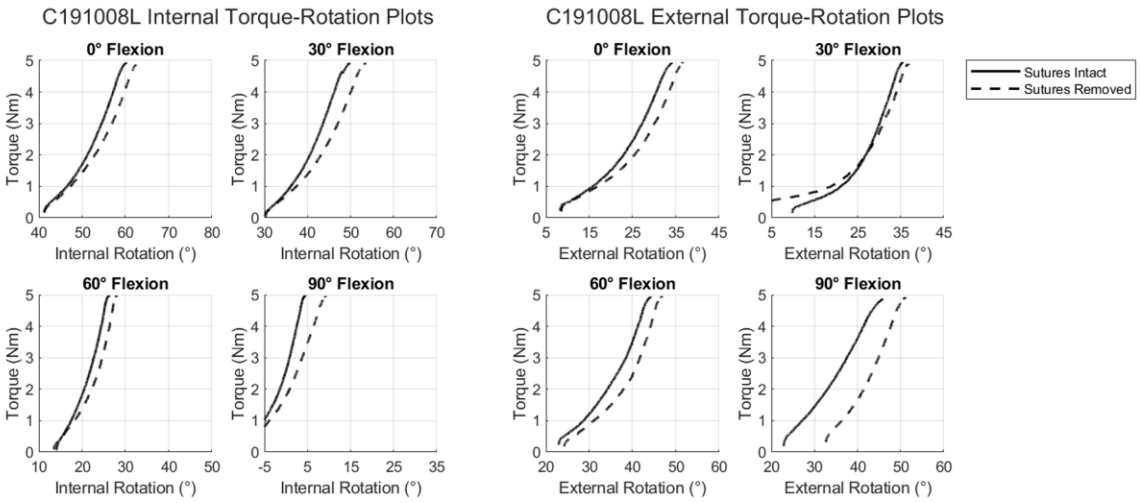

Figure C.3: Specimen C191008L Internal & External Torque-Rotation Curves at Various Flexion Angles

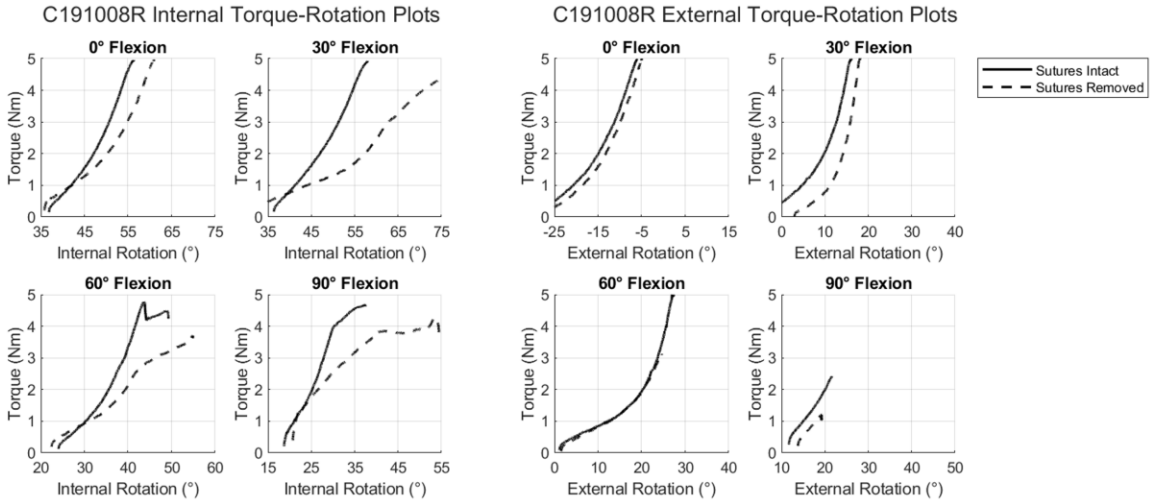

Figure C.4: Specimen C191008R Internal & External Torque-Rotation Curves at Various Flexion Angles

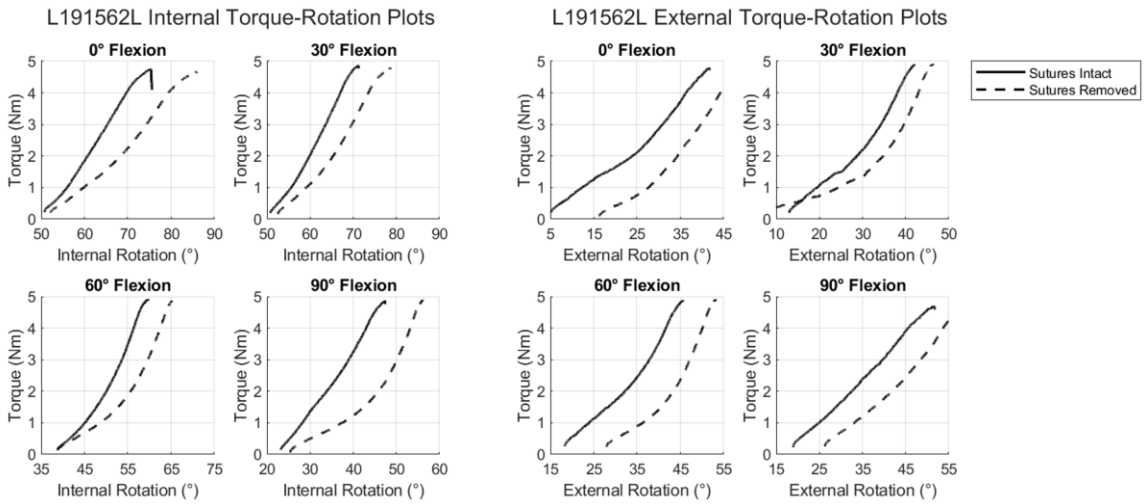

Figure C.5: Specimen L191562L Internal & External Torque-Rotation Curves at Various Flexion Angles

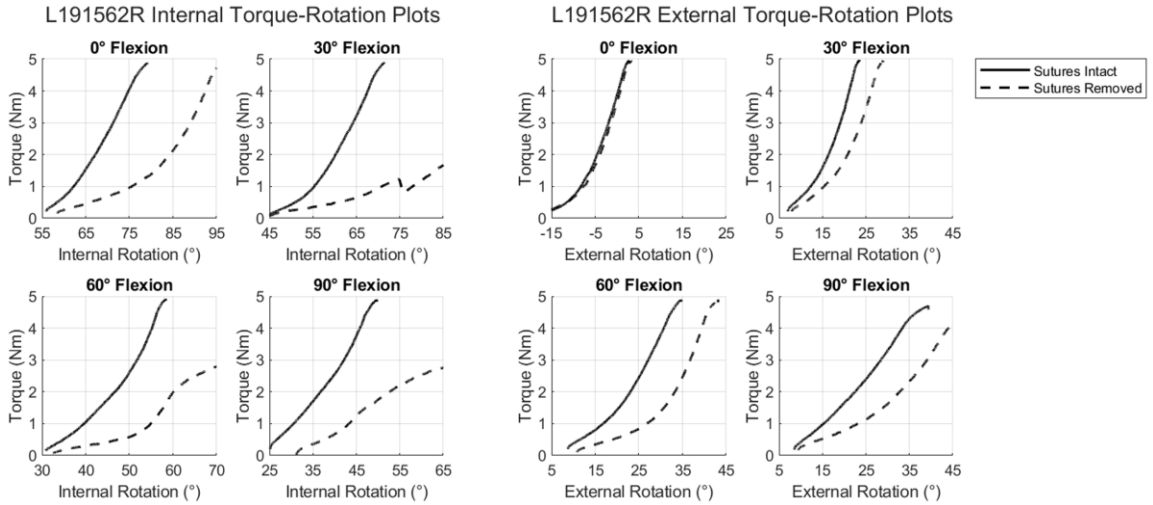

Figure C.6: Specimen L191562R Internal & External Torque-Rotation Curves at Various Flexion Angles

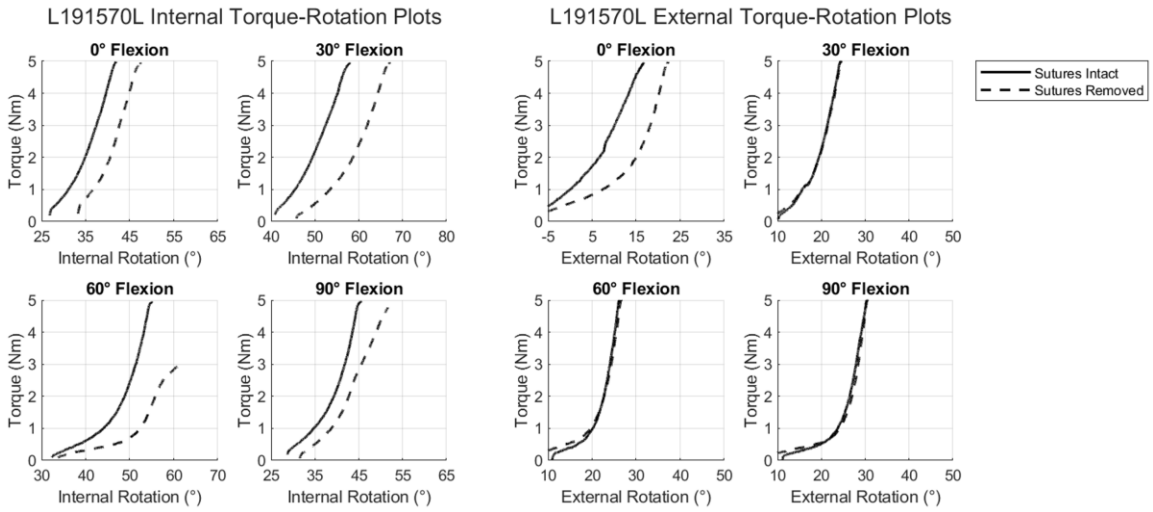

Figure C.7: Specimen L191570L Internal & External Torque-Rotation Curves at Various Flexion Angles

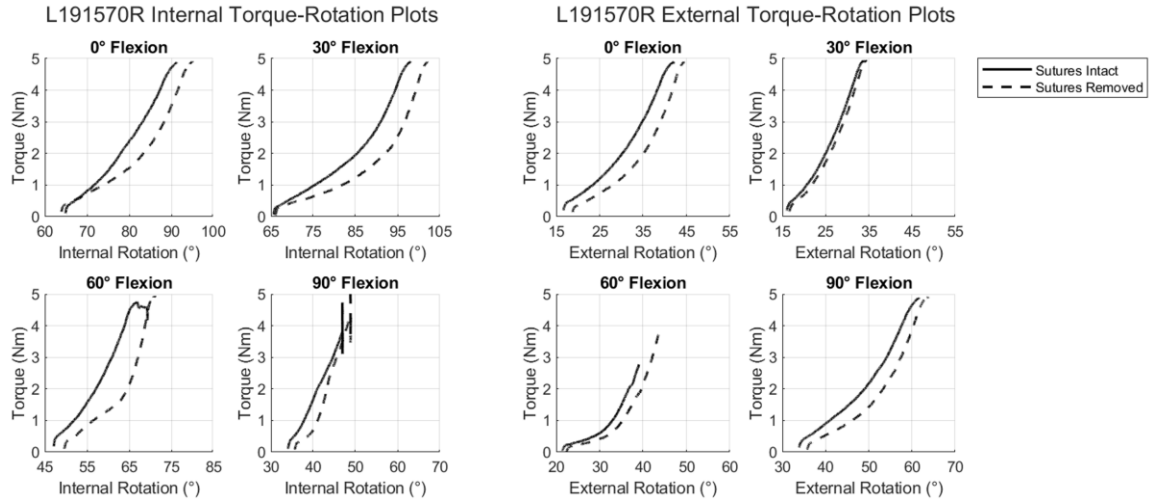

Figure C.8: Specimen L191570R Internal & External Torque-Rotation Curves at Various Flexion Angles

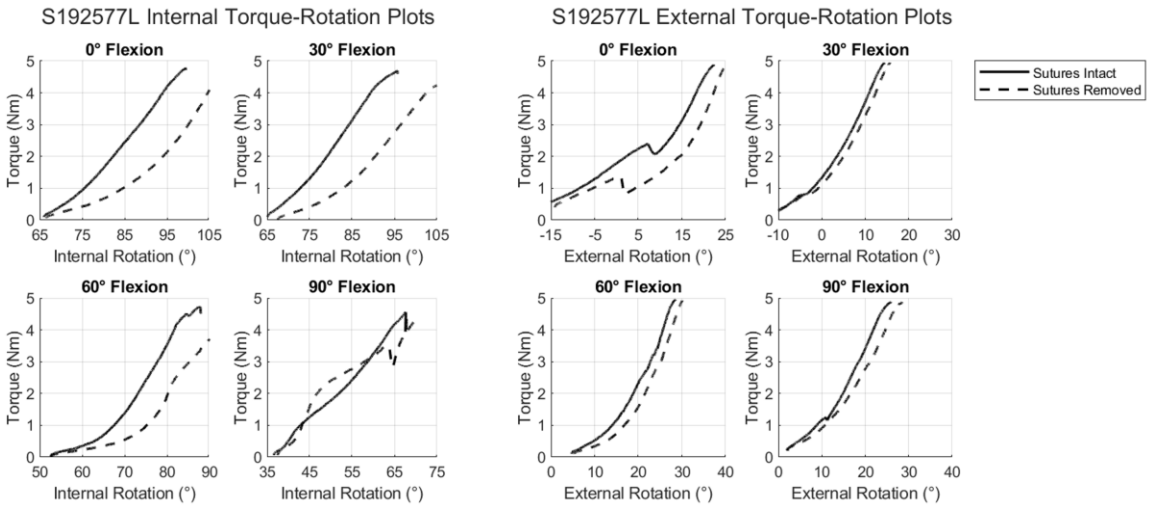

Figure C.9: Specimen S192577L Internal & External Torque-Rotation Curves at Various Flexion Angles

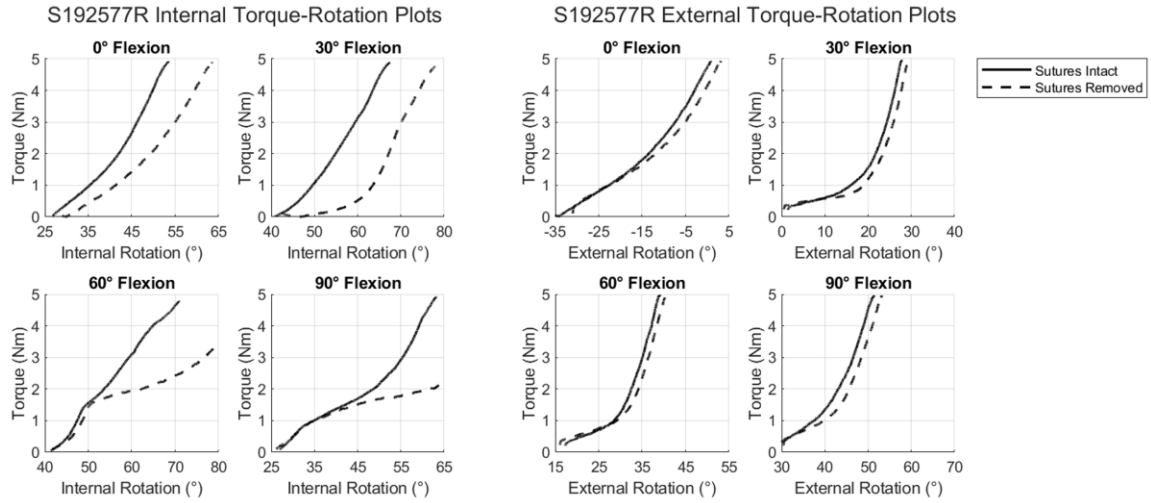

Figure C.10: Specimen S192577R Internal & External Torque-Rotation Curves at Various Flexion Angles

Appendix D: Sutures Intact and Sutures Removed Dislocation Plots

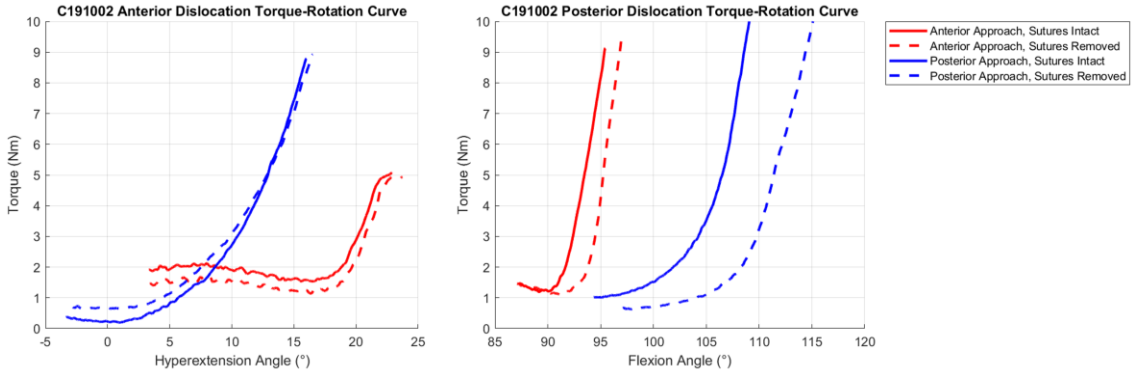

Figure D.1: Specimen C191002 Anterior and Posterior Dislocation Torque-Rotation Curves (Sutures Intact/Removed)

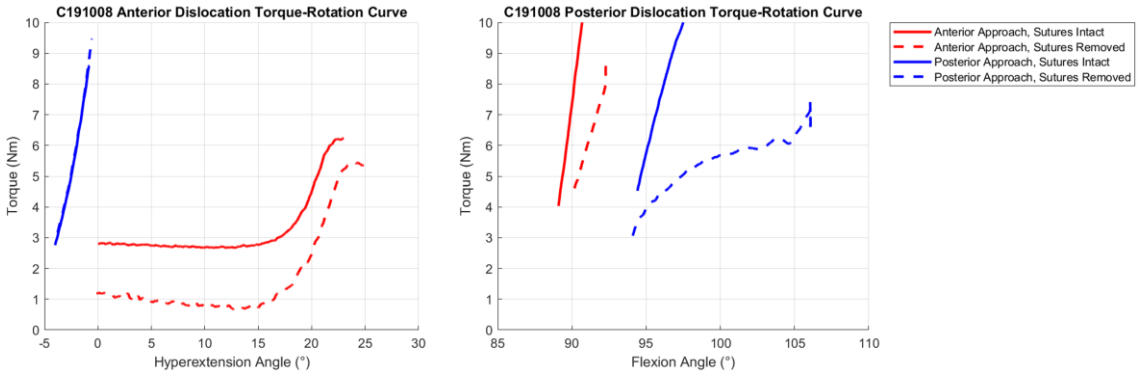

Figure D.2: Specimen C191008 Anterior and Posterior Dislocation Torque-Rotation Curves (Sutures Intact/Removed)

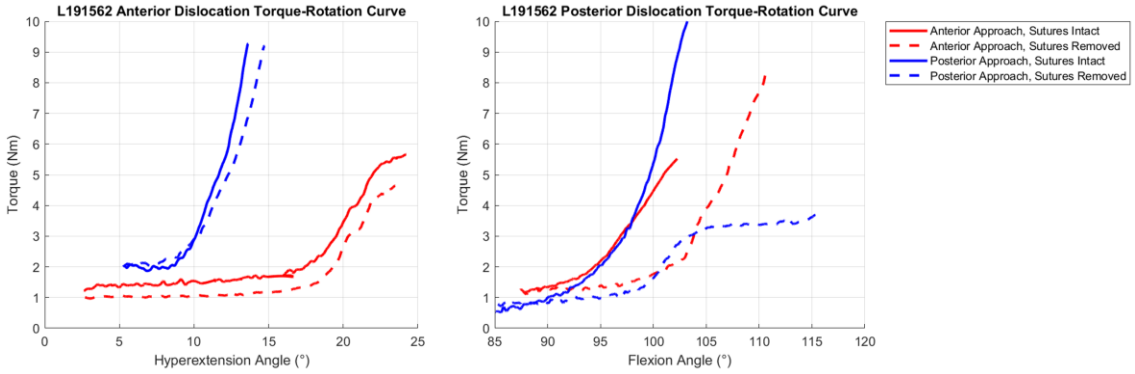

Figure D.3: Specimen L191562 Anterior and Posterior Dislocation Torque-Rotation Curves (Sutures Intact/Removed)

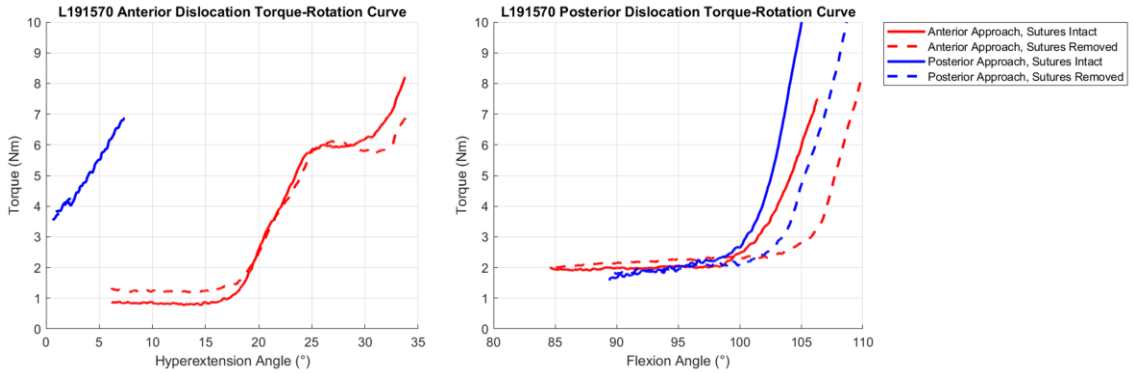

Figure D.4: Specimen L191570 Anterior and Posterior Dislocation Torque-Rotation Curves (Sutures Intact/Removed)

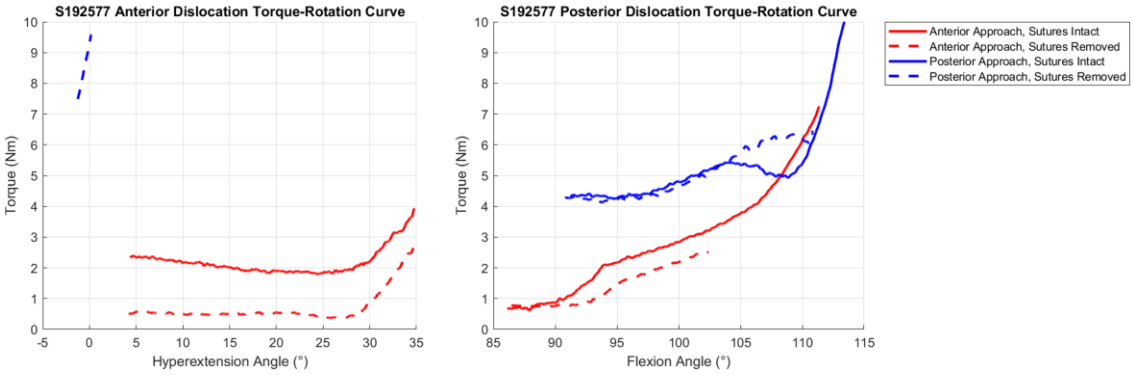

Figure D.5: Specimen S192577 Anterior and Posterior Dislocation Torque-Rotation Curves (Sutures Intact/Removed)

Appendix E: DM- and c-THA Dislocation Plots

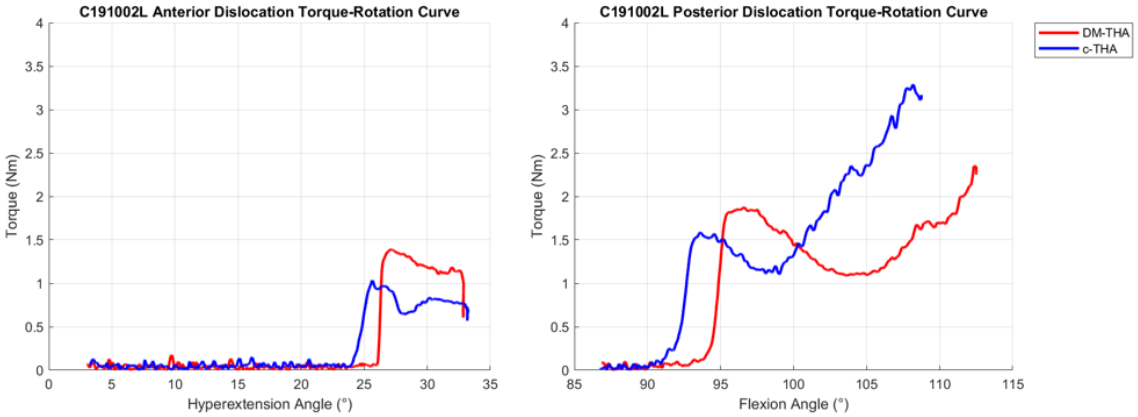

Figure E.1: Specimen C191002L Anterior and Posterior Dislocation Torque-Rotation Curves (Skeletonized DM-/c-THA)

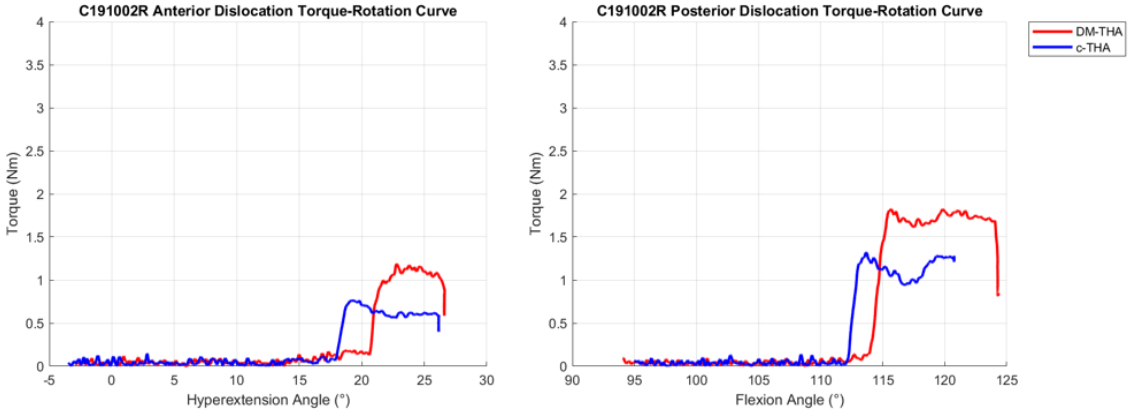

Figure E.2: Specimen C191002R Anterior and Posterior Dislocation Torque-Rotation Curves (Skeletonized DM-/c-THA)

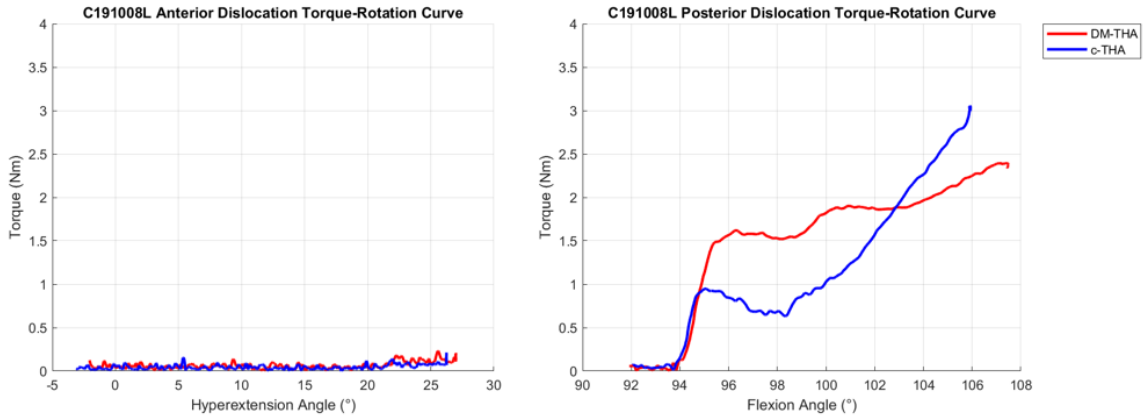

Figure E.3: Specimen C191008L Anterior and Posterior Dislocation Torque-Rotation Curves (Skeletonized DM-/c-THA)

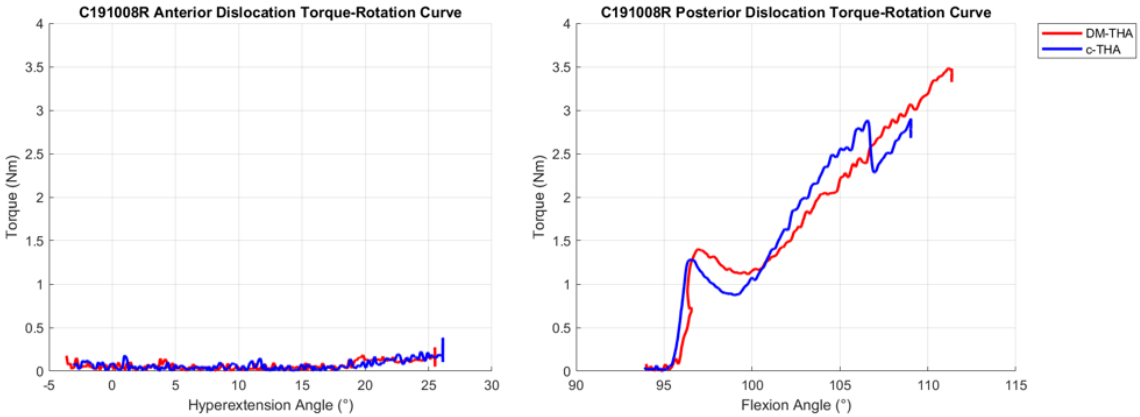

Figure E.4: Specimen C191008R Anterior and Posterior Dislocation Torque-Rotation Curves (Skeletonized DM-/c-THA)

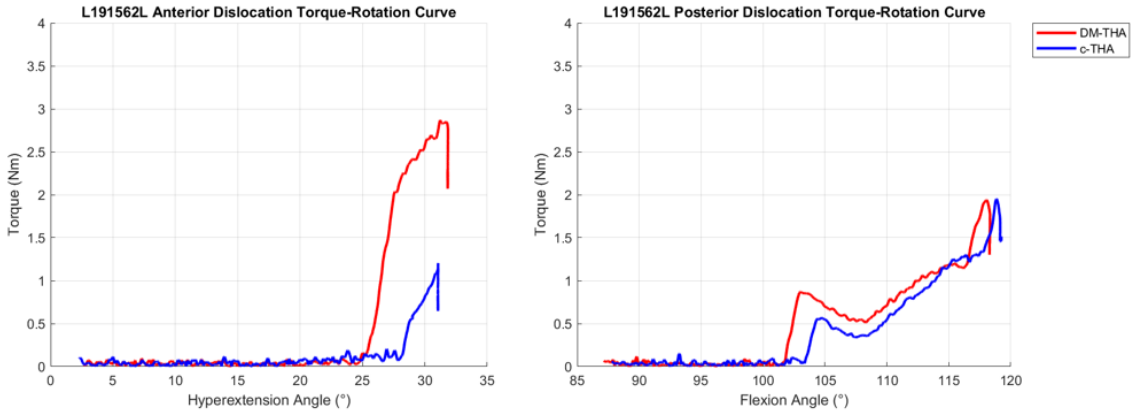

Figure E.5: Specimen L191562L Anterior and Posterior Dislocation Torque-Rotation Curves (Skeletonized DM-/c-THA)

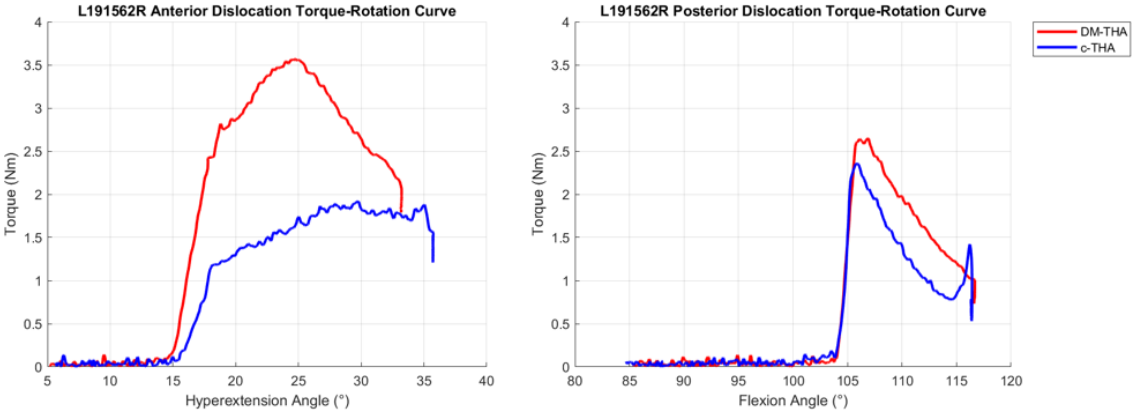

Figure E.6: Specimen L191562R Anterior and Posterior Dislocation Torque-Rotation Curves (Skeletonized DM-/c-THA)

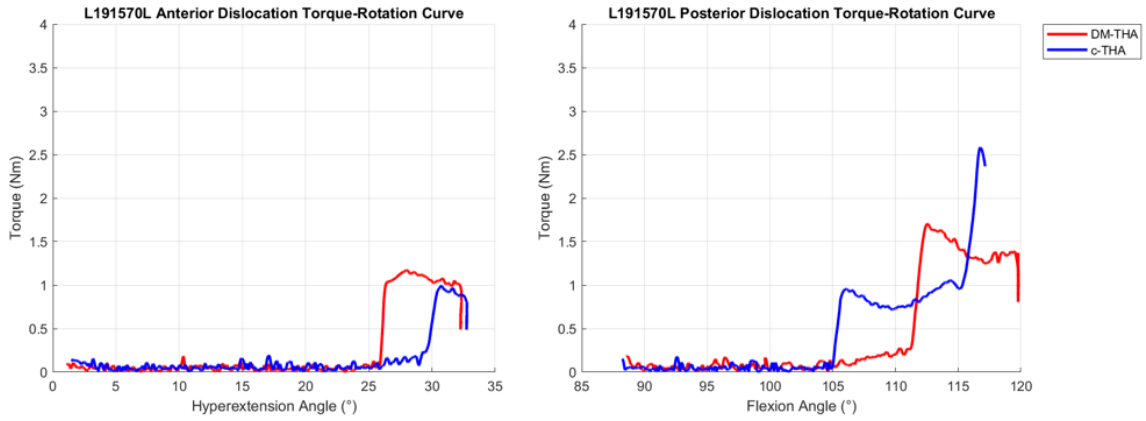

Figure E.7: Specimen L191570L Anterior and Posterior Dislocation Torque-Rotation Curves (Skeletonized DM-/c-THA)

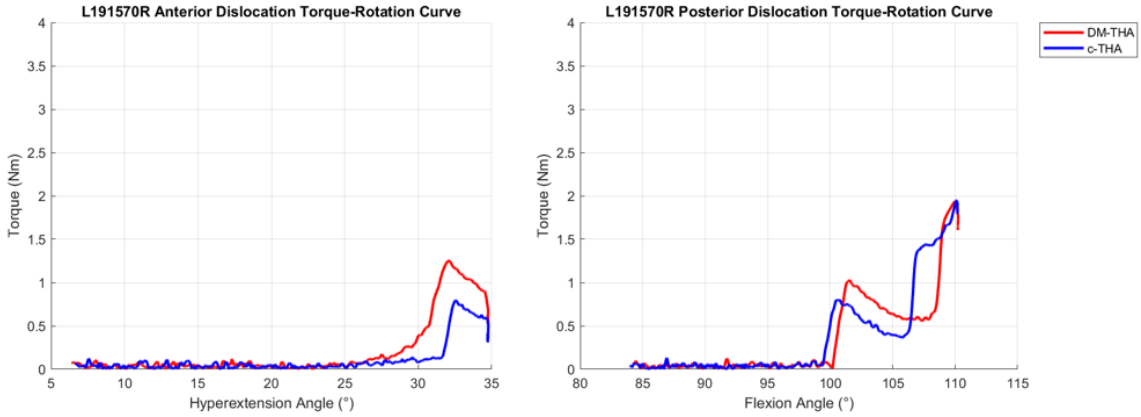

Figure E.8: Specimen L191570R Anterior and Posterior Dislocation Torque-Rotation Curves (Skeletonized DM-/c-THA)

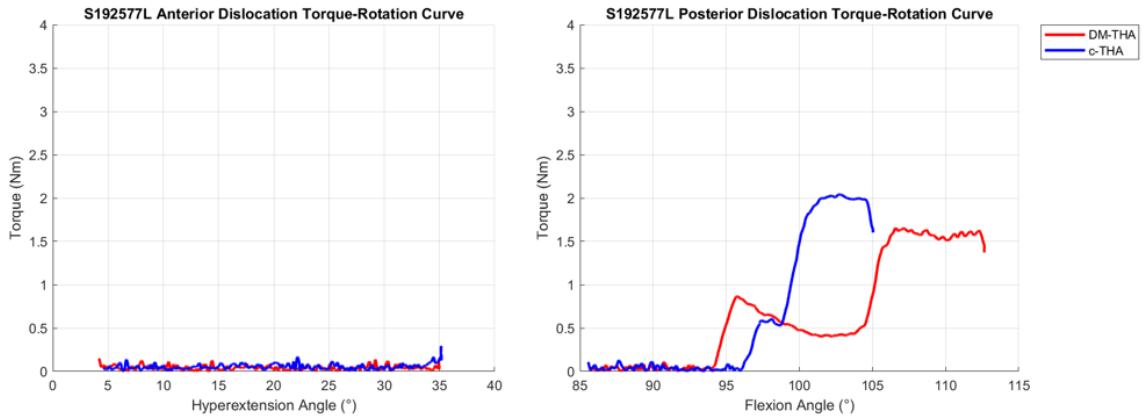

Figure E.9: Specimen S192577L Anterior and Posterior Dislocation Torque-Rotation Curves (Skeletonized DM-/c-THA)

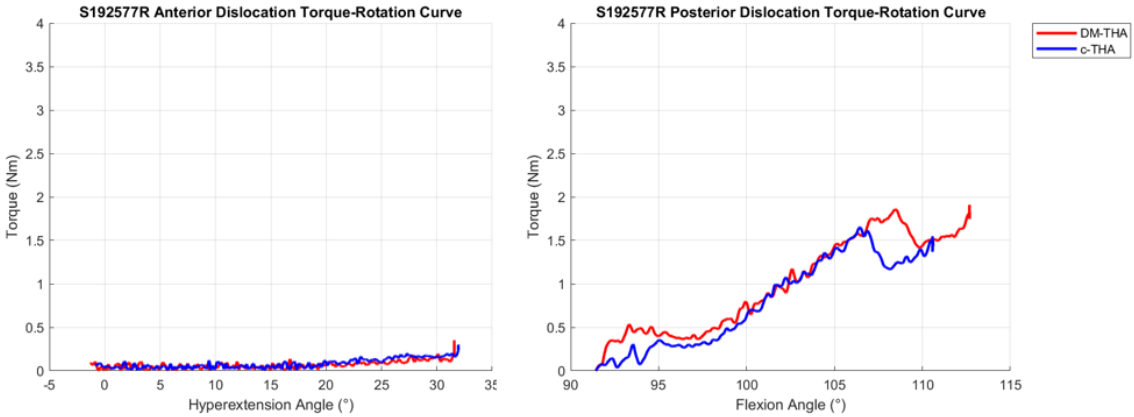

Figure E.10: Specimen S192577R Anterior and Posterior Dislocation Torque-Rotation Curves (Skeletonized DM-/c-THA)